1. Report No.	2. Government Accession No.	3. Recipient's Catalog No.
SWUTC/07/167264-1		

4. Title and Subtitle	5. Report Date
Calibration of Pavement Response Models for the Mechanistic-Empirical Pavement Design Method	September 2007
	6. Performing Organization Code

7. Author(s)	8. Performing Organization Report No.
Rong Luo and Jorge A. Prozzi	SWUTC/07/167264-1

9. Performing Organization Name and Address	10. Work Unit No. (TRAIS)
Center for Transportation Research University of Texas at Austin 3208 Red River, Suite 200 Austin, Texas 78705-2650	11. Contract or Grant No. 10727

12. Sponsoring Agency Name and Address	13. Type of Report and Period Covered
Southwest Region University Transportation Center Texas Transportation Institute Texas A&M University System College Station, Texas 77843-3135	Research Report September 1, 2006 – August 31, 2007
	14. Sponsoring Agency Code

15. Supplementary Notes

Supported by general revenues from the State of Texas.

16. Abstract

Most pavement design methodologies assume that the tire-pavement contact stress is equal to the tire inflation pressure and uniformly distributed over a circular contact area. However, tire-pavement contact area is not in a circular shape and the contact stress is neither uniform nor equal to the tire inflation pressure.

To precisely account for the effect of actual contact stress on pavement responses, this research evaluates pavement responses under the 3-D non-uniform stresses and under the uniform stress. The studied pavement responses include the horizontal strains at the pavement surface, the horizontal strains at the bottom of the asphalt layer, and the vertical strains at the top of subgrade. A multi-layer linear-elastic computer program, CIRCLY, is used to estimate pavement strains under a number of combinations of tire load, tire pressure, asphalt modulus, asphalt thickness and subgrade modulus. The Asphalt Institute method and the Shell method are used to predict the pavement fatigue life based on the critical strains at the bottom of the asphalt layer calculated by both 3-D stress model and the uniform stress model.

Results show that the vertical contact stress component of the 3-D stresses has the dominant effect on the studied pavement strains. The effects of longitudinal stress component and the transverse stress component cannot be ignored, especially for pavement with a thin asphalt layer. Asphalt thickness, asphalt modulus, tire load and tire pressure have significant effects on the differences in asphalt strains between the 3-D stress model and the uniform stress model, but not on the difference in the vertical strains at the subgrade top. Subgrade modulus shows little effect on the differences in all studied strains predicted by the 3-D stress model and the uniform stress model. Tire pressure has greater effect than tire load on the fatigue life of a pavement with a thin asphalt layer. When the pavement has a thick asphalt layer, the effect of tire load is greater than the effect of tire pressure, and a larger tire load is associated with a smaller number of load repetitions.

17. Key Words	18. Distribution Statement
Mechanistic-Empirical Design, Wheel Load, Tire Pressure, Pavement Response, Non-Uniform Contact Stress	No restrictions. This document is available to the public through NTIS: National Technical Information Service 5285 Port Royal Road Springfield, Virginia 22161

19. Security Classif.(of this report)	20. Security Classif.(of this page)	21. No. of Pages	22. Price
Unclassified	Unclassified	85	

Calibration of Pavement Response Models for the Mechanistic-Empirical Pavement Design Method

By
Rong Luo
Jorge A. Prozzi

Research Report SWUTC/07/167264-1

Southwest Region University Transportation Center
Center for Transportation Research
University of Texas at Austin
Austin, Texas 78712

September 2007

ABSTRACT

Most pavement design methodologies assume that the tire-pavement contact stress is equal to the tire inflation pressure and uniformly distributed over a circular contact area. However, tire-pavement contact area is not in a circular shape and the contact stress is neither uniform nor equal to the tire inflation pressure.

To precisely account for the effect of actual contact stress on pavement responses, this research evaluates pavement responses under the 3-D non-uniform stresses and under the uniform stress. The studied pavement responses include the horizontal strains at the pavement surface, the horizontal strains at the bottom of the asphalt layer, and the vertical strains at the top of subgrade. A multi-layer linear-elastic computer program, CIRCLY, is used to estimate pavement strains under a number of combinations of tire load, tire pressure, asphalt modulus, asphalt thickness and subgrade modulus. The Asphalt Institute method and the Shell method are used to predict the pavement fatigue life based on the critical strains at the bottom of the asphalt layer calculated by both 3-D stress model and uniform stress model.

Results show that the vertical contact stress component of the 3-D stresses has the dominant effect on the studied pavement strains. The effects of longitudinal stress component and the transverse stress component cannot be ignored, especially for pavement with a thin asphalt layer. Asphalt thickness, asphalt modulus, tire load and tire pressure have significant effects on the differences in asphalt strains between the 3-D stress model and the uniform stress model, but not on the difference in the vertical strains at the subgrade top. Subgrade modulus shows little effect on the differences in all studied strains predicted by the 3-D stress model and the uniform stress model. Tire pressure has greater effect than tire load on the fatigue life of a pavement with a thin asphalt layer. When the pavement has a thick asphalt layer, the effect of tire load is greater than the effect of tire pressure, and a larger tire load is associated with a smaller number of load repetitions.

EXECUTIVE SUMMARY

Fatigue cracking and rutting are two major distresses of flexible pavements. Fatigue cracking includes: 1) bottom-up cracking, which initiates at the bottom of the asphalt layer and propagates to the surface; and 2) top-down cracking, which starts from the pavement surface and develops downward. Rutting is the depression at pavement surface arising from the permanent deformation in any of the pavement layers or the subgrade. To predict these pavement distresses, most pavement design methods, such as the Mechanistic-Empirical Pavement Design Guide developed by the National Cooperative Highway Research Program, use pavement distress models (transfer functions) in terms of layer stiffness or modulus and pavement responses. Critical pavement responses are particularly interesting because they are required as inputs into the transfer functions. Therefore, the bottom-up or top-down cracking is predicted based on the maximum tensile strain in the horizontal direction at the bottom or top of the asphalt layer, and the permanent deformation of the subgrade is estimated by using the maximum vertical strain at the top of the subgrade. These critical pavement responses used in the distress models are calculated in the pavement response models by applying vertical tire-pavement contact stress to the pavement surface. The contact stress is typically assumed to be equal to the tire inflation pressure and to be uniformly distributed over a circular contact area in the vertical direction. The radius of the circular contact area is calculated based on the wheel load and tire inflation pressure.

However, it has been recognized that the tire-pavement contact area is not in a circular shape and that the contact stress is neither uniform nor equal to the tire inflation pressure. Recent research has quantified the actual contact stress distributed in a three-dimensional (3-D) space. The three components of contact stress are vertical stress, longitudinal stress and transverse stress. All three stress components can be measured by the Vehicle-Road-Surface-Pressure-Transducer-Array (VRSPTA) system. Vertical stress is considered the predominant factor in pavement response. Researchers have applied the measured 3-D non-uniform contact stresses to the pavement surface to predict critical pavement responses, and have reported significant differences in the predicted pavement responses between the traditional uniform contact stress model and the non-uniform stress model. However, these findings were limited to specific

pavement structures with a small range of layer thickness and stiffness. An earlier study indicated that the conventional uniform stress model did not overestimate or underestimate pavement response for all pavement structures. For certain combinations of tire loading, tire pressure and asphalt thickness, the uniform stress model produces similar results as the non-uniform stress model. In addition, the moduli of pavement layers may have significant effects in the comparison of the two models. Another important limitation is that transfer functions that account for the effect of the 3-D stresses have not been developed. Therefore, it is necessary to study all variables of which the pavement responses are dependent, including wheel load, tire inflation pressure, layer thickness and layer modulus. These variables need to be quantified and scientifically related to calibrate the traditional uniform stress model.

This research incorporates the measured 3-D non-uniform tire-pavement contact stresses as well as the traditional uniform contact stresses to study pavement responses and performance. Multi-layer linear elastic program, CIRCLY, is used to simulate measured 3-D stress and uniform stress. The experimental design includes five variables: i) 12 asphalt layer thicknesses; ii) five levels of tire load; iii) five levels of tire pressure; iv) five levels of asphalt modulus; and v) five levels of subgrade modulus.

The analysis evaluates the individual and combined effects of the 3-D stress components (vertical stress, longitudinal stress and transverse stress) on the distributions of pavement strains within and close to the contact area at pavement surface, the bottom of the asphalt layer, and the top of subgrade. The studied pavement strains include: i) longitudinal and transverse strains at pavement surface; ii) longitudinal and transverse strains at the bottom of the asphalt layer; and iii) vertical strains at the top of subgrade. Every strain distribution is graphically presented in three dimensions using MATLAB software. The strain distributions as well as the critical values of all strain distributions calculated by the 3-D stress model are compared to those estimated by the uniform stress model in order to evaluate the possible errors caused by the assumptions in the traditional uniform stress model.

Two pavement distress models, the Asphalt Institute method and the Shell method, are used to predict pavement fatigue life based on the tensile strains calculated by both 3-D stress model and

the uniform stress model. The pavement fatigue life results predicted by the Asphalt Institute method are analyzed in detail. The fatigue life results predicted by the Shell method are plotted in Appendix 2. The effects of tire load and tire pressure on pavement fatigue life are reported and compared at different asphalt thickness levels.

The major findings of this study are summarized as follows:

- Among the three stress components of the measured 3-D contact stresses, the vertical stress has the dominant effect on the horizontal strains in both directions at pavement surface and at the bottom of the asphalt layer, and on the vertical strains at the top of subgrade. Although the effects of longitudinal stress component and transverse stress component are secondary to the effect of the vertical stress component, they are significant and cannot be ignored, especially for thinner pavements which constitute the vast majority of Texas' road network.
- Under the 3-D stresses, both longitudinal and transverse strains at the pavement surface are compressive strains within the contact area and are tensile strains at the edge or adjacent to the contact area. As the asphalt thickness increases, the horizontal tensile strains tend to decrease under the combined effect of 3-D stresses.
- Under the 3-D stresses, when the asphalt layer is relatively thin, two peaks of tensile strain distribution develop at the bottom of the asphalt layer within the contact area, and compressive strains develop at the edge and outside of the contact area. The compressive strain may develop around the center of the contact area for pavement with a very thin asphalt layer. As the asphalt thickness increases, the shape of the transverse strain distribution changes from a "w-shape" to a "u-shape".
- Asphalt modulus, asphalt thickness, tire load and tire pressure have significant effect on the differences in strains at pavement surface and at the bottom of the asphalt between the 3-D stress model and the uniform stress model, but not on the differences in strains at the top of subgrade. Subgrade modulus has a slight effect on the differences in all pavement strains predicted by the 3-D stress model and the uniform stress model.

Tire pressure shows significant effect on the fatigue life of a pavement with a thin asphalt layer. The effect of tire pressure decreases as the asphalt thickness increases. When the asphalt thickness is small, a higher tire load is associated with a larger number of load repetitions in most cases. When the pavement has a thick asphalt layer, a higher tire load is accompanied by a smaller number of load repetitions, and the effect of tire load is larger than the effect of tire pressure.

TABLE OF CONTENTS

LIST OF FIGURES

LIST OF TABLES

DISCLAIMER

The contents of this report reflect the views of the authors, who are responsible for the facts and the accuracy of the information presented herein. This document is disseminated under the sponsorship of the Department of Transportation, University Transportation Centers Program, in the interest of information exchange. Mention of trade names or commercial products does not constitute endorsement or recommendation for use.

ACKNOWLEDGEMENTS

The authors recognize that support for this research was provided by a grant from the U.S. Department of Transportation, University Transportation Centers Program to the Southwest Region University Transportation Center which is funded, in part, with general revenue funds from the State of Texas.

Chapter 1 Introduction

1.1 Research Motivation

Fatigue cracking and rutting are two major distresses of flexible pavements. Fatigue cracking includes (El-basyouny and Witczak, 2005): 1) bottom-up cracking, which initiates at the bottom of the asphalt layer and propagates to the surface; and 2) top-down cracking, which starts from the pavement surface and develops downward. Rutting is the depression at pavement surface arising from the permanent deformation in any of the pavement layers or the subgrade. To predict these pavement distresses, most pavement design methods, such as the Mechanistic-Empirical Pavement Design Guide developed by the National Cooperative Highway Research Program (NCHRP), use pavement distress models (transfer functions) in terms of layer stiffness or modulus and pavement responses. Critical pavement responses are particularly interesting because they are required as inputs into the transfer functions. Therefore, the bottom-up or top-down cracking is predicted based on the maximum tensile strain in the horizontal direction at the bottom or top of the asphalt layer, and the permanent deformation of the subgrade is estimated by using the maximum vertical strain at the top of the subgrade. These critical pavement responses used in the distress models are calculated in the pavement response models by applying vertical tire-pavement contact stress to the pavement surface. The contact stress is typically assumed to be equal to the tire inflation pressure and to be uniformly distributed over a circular contact area in the vertical direction. The radius of the circular contact area is calculated based on the wheel load and tire inflation pressure.

However, it has been recognized that the tire-pavement contact area is not in a circular shape and that the contact stress is neither uniform nor equal to the tire inflation pressure. Recent research has quantified the actual contact stress distributed in a three-dimensional (3-D) space (De Beer et al., 1997; De Beer and Fisher, 2002; De Beer, 2006). The three components of contact stress are vertical stress, longitudinal stress and transverse stress. All three stress components can be measured by the Vehicle-Road-Surface-Pressure-Transducer-Array (VRSPTA) system. Vertical stress is considered the predominant factor in pavement response. Researchers have applied the measured 3-D non-uniform contact stresses to the pavement surface to predict critical pavement

responses (Prozzi and Luo, 2005; Machemehl et al., 2005; Luo and Prozzi, 2007). They have reported significant differences in the predicted pavement responses between the traditional uniform contact stress model and the non-uniform stress model. However, these findings were limited to specific pavement structures with a small range of layer thickness and stiffness. An earlier study indicated that the conventional uniform stress model did not overestimate or underestimate pavement response for all pavement structures. For certain combinations of tire loading, tire pressure and asphalt thickness, the uniform stress model produces similar results as the non-uniform stress model. In addition, the moduli of pavement layers may have significant effects in the comparison of the two models. Another important limitation is that transfer functions that account for the effect of the 3-D stresses have not been developed. Therefore, it is necessary to study all variables of which the pavement responses are dependent, including wheel load, tire inflation pressure, layer thickness and layer modulus. These variables need to be quantified and scientifically related to calibrate the traditional uniform stress model.

1.2 Report Outline

The following chapter details the modeling of the 3-D non-uniform contact stresses and the uniform contact stress. The measurement of the 3-D contact stresses will be introduced, and the experimental variables in this study will be selected based on engineering judgment. A computer program, CIRCLY, will be used to model the 3-D stresses and the uniform stress. The modeling process is detailed in Chapter 2.

Chapter 3 will present typical pavement strains calculated by the 3-D stress model and the uniform stress model. Pavement strain distributions at specific locations will be graphically illustrated. The critical pavement strains computed by the 3-D stress model will be compared to those predicted by the uniform stress model in order to identify possible errors in the uniform stress model caused by the traditional assumptions on tire-pavement contact conditions. This chapter will also discuss the effects of experimental variables on the differences in critical pavement strains between the 3-D stress model and the uniform stress model.

Chapter 4 will use two pavement distress models to predict the pavement fatigue life under different combinations of tire load, tire pressure and asphalt thickness. The pavement fatigue life calculated based on the tensile strains from the 3-D stress model will be compared to that computed based on the tensile strains from the uniform stress model. The effects of tire load, tire pressure and asphalt thickness on the pavement fatigue life will be analyzed and compared.

Chapter 5 will summarize the major findings of this research.

Chapter 2 Modeling of Pavement under Tire-Pavement Contact Stresses

2.1 Measurement of Tire-Pavement Contact Stress

The Council of Scientific and Industrial Research (CSIR) of South Africa used the SIM Mk IV system to measure the 3-D tire-pavement contact stresses under two tire types for the Texas Department of Transportation (TxDOT) (De Beer and Fisher, 2002). The SIM Mk IV system consisted of four SIM pad assemblies, one of which was used for this test. An array of 21 instrumented pins crossing the center of the SIM pad assembly measured 3-D forces applied by the tire as it was moving over the SIM at a low speed. Each pin measured the longitudinal, transverse and vertical forces at a frequency of 1001 Hz. This high frequency ensured that the instrumented pins captured a large number of SIM data (the distance of adjacent data rows was only 0.35mm), which allowed data reduction, if needed, without compromising accuracy. Besides the instrumented pins, each SIM pad had approximately 1041 supporting pins on both sides of the instrumented pins to support the test tire. The center-to-center distance between the adjacent pins was 17 mm.

The test tires were a new Goodyear 11R24.5 G G159A and a new Goodyear 215/75R17.5 H G114, both of which were tested in a total of 25 different combinations of target wheel load and tire inflation pressure. The load was hydraulically applied using the Heavy Vehicle Simulator (HVS) Mk III, and the wheel speed was approximately 0.350 m/s during the test. The data of the SIM measurements were electronically presented in .txt format and graphically illustrated in .jpg format generated by MATLAB (De Beer and Fisher, 2002). This research uses the contact stress data for one tire in the above test, the Goodyear 11R24.5 G G159A, which is one of the most popular tires used in Texas.

In general, the vertical stress component measured in the test is higher in magnitude than the other two stress components. However, longitudinal stress and transverse stress are still significant because at some locations, the absolute values of the longitudinal stress and the transverse stress are as high as 55% and 25% of the vertical stress, respectively. In addition, unlike the vertical stresses, all of which are compressive within the contact area, longitudinal

stresses and transverse stresses may be in either tension or compression at different positions. These two stress components may have a significant effect on the horizontal strains in the asphalt layer, especially for a pavement with a relatively thin asphalt layer. As a result, the separate effect of the three stress components as well as the combined effect of the 3-D stresses will be investigated in the following sections.

2.2 Experimental Variables

The experimental analysis includes five variables: wheel load, tire inflation pressure, asphalt thickness, asphalt modulus, and subgrade modulus. The variable of asphalt thickness has twelve values, while each of the other four variables has five levels of magnitude. In total, 7,500 cases are studied in the experimental design.

The target tire loading varies from 20.4 kN (4590 lb) to 34.6 kN (7785 lb), while the tire inflation pressure ranges from 483 kPa (70 psi) to 896 kPa (130 psi). In the contact stress test at CSIR of South Africa, the actual applied load was slightly different from the target loading at each load level. Table 2.1 summarizes the 25 combinations of tire loading and tire inflation pressure, in which "L" represents the tire loading level and "P' symbolizes the tire pressure level. For example, "L1P1" means the combination of the first load level (20.4 kN) and the first tire pressure level (483 kPa).

Table 2.1 Twenty-five Combinations of Target Tire Loading and Tire Inflation Pressure

Tire Inflation Pressure (kPa / psi)	Target Wheel Load (kN / lb)				
	20.4 / 4590	**24.0 / 5400**	**27.5 / 6187.5**	**31.1 / 6997.5**	**34.6 / 7785**
483 / 70	L1P1	L2P1	L3P1	L4P1	L5P1
586 / 85	L1P2	L2P2	L3P2	L4P2	L5P2
690 / 100	L1P3	L2P3	L3P3	L4P3	L5P3
793 / 115	L1P4	L2P4	L3P4	L4P4	L5P4
896 / 130	L1P5	L2P5	L3P5	L4P5	L5P5

Typical pavement structures in Texas are selected for the experimental design. All the pavement structures consist of an asphalt layer, base, subbase and subgrade. Each layer is assumed to be homogenous, isotropic and linearly elastic with a Poisson's ratio of 0.35. The variable of asphalt modulus has five values: 1,500, 2,500, 3,500, 4,500 and 5,500 MPa. The subgrade modulus has a

range of 25, 50, 75, 100 and 125 MPa. The base and subbase have constant modulus values of 500 MPa and 250 MPa, respectively. The thickness of the asphalt layer, the fifth variable, has twelve values in this study. Either base or subbase has a constant thickness. Table 2.2 details the selected pavement structures. A total of 300 combinations of pavement structures are studied in this research, which covers a large range of pavement types with different layer thicknesses and material properties.

Table 2.2 Selected Pavement Structures

Pavement Layer	Construction Material	Thickness (mm / in.)	Young's Modulus (MPa / psi)
Asphalt Layer	Dense Asphalt	25 / 1.0	1,500 / 217
		40 / 1.6	
		55 / 2.2	2,500 / 362
		70 / 2.8	
		85 / 3.3	3,500 / 507
		100 / 3.9	
		115 / 4.5	4,500 / 652
		130 / 5.1	
		160 / 6.3	5,500 / 797
		190 / 7.5	
		220 / 8.7	
		250 / 9.8	
Base	A-1-b Base	250 / 9.8	500 / 72
Subbase	A-2-4 Subbase	250 / 9.8	250 / 36
Subgrade	A-6 Subgrade	Infinite	25 / 4
			50 / 7
			75 / 11
			100 / 15
			125 / 18

2.3 Simulation of 3-D Stress

A multi-layer linearly elastic (LE) program, CIRCLY, is used to model the measured 3-D tire-pavement contact stresses. CIRCLY requires much less computation effort and time without significant loss of accuracy compared to alternative finite element (FE) programs. Machemehl et al. (2005) verified that with accurate modeling, such as that proposed in this study, the difference in strain estimation between FE and LE programs is negligible. Both CIRCLY and ANSYS were used to calculate the responses of a randomly selected pavement structure under the non-uniform contact stresses measured by De Beer and Fisher (1997). The researchers reported that CIRCLY completed a single run in only one to two minutes while it took ANSYS approximately one hour

to compute the same problem on the same computer. To store the computation results, CIRCLY used only 50 KB while ANSYS occupied 1.4 GB of disk space. By comparison, it was shown that the results produced by the two programs matched very well for critical results at various pavement depths except locations close to the pavement surface (<20 mm) where appreciable differences were found. This observation indicates that CIRCLY is reliable and much more economical than the FE programs in evaluating the responses of linearly elastic pavement structures.

CIRCLY can model load only in a circular shape. The parameters needed for input into CIRCLY include: i) circular load with radius, stress and location; ii) layered pavement system characterized by layer thickness, interface type, and mechanical properties (Poisson's ratio and Young's modulus); and iii) locations to be analyzed within the pavement structure. CIRCLY can model six different types of loading stress distributions applied to circular areas, as shown in Figure 2.1. Each load type corresponds to a typed code from 1 through 6 in CIRCLY. In this study, Load Type 1 (Vertical Force, Figure 2.1 (a)) and Load Type 2 (Horizontal Force, Figure 2.1 (b)) are used to simulate the vertical stress and horizontal stress (including the longitudinal stress and transverse stress), respectively.

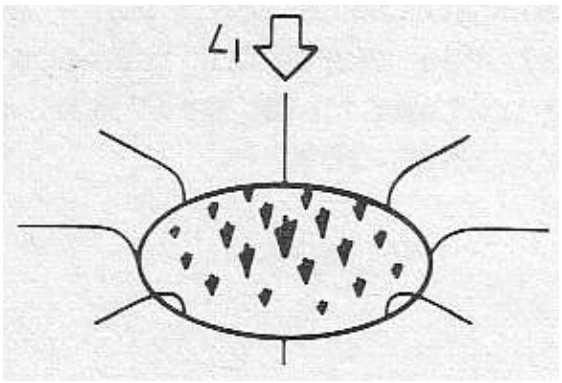

(a) Vertical Force

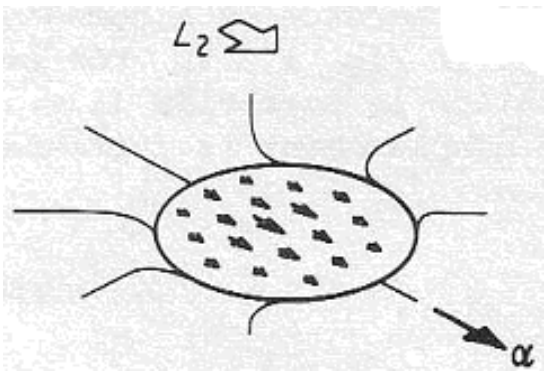

(b) Horizontal Force

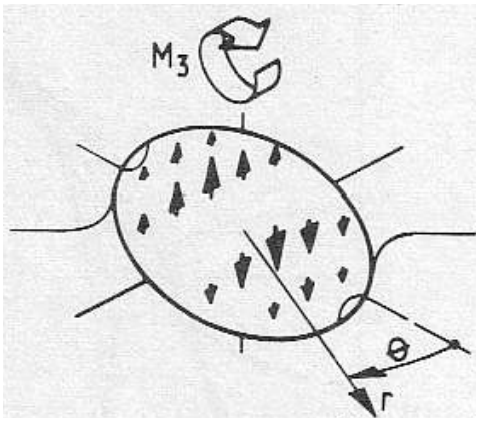

(c) Moment about Horizontal Axis

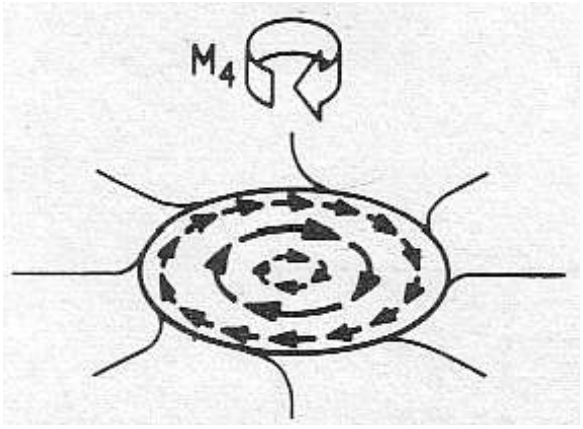

(d) Moment about Vertical Axis

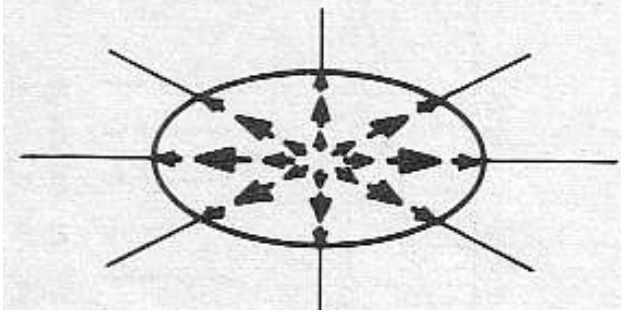

(e) Radial Shear Stress

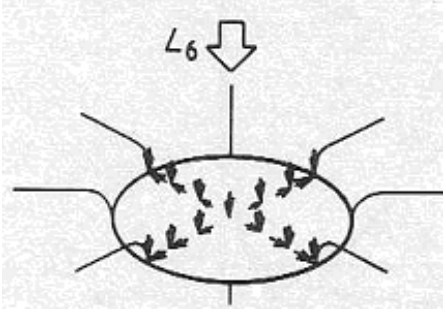

(f) Vertical Force (Rough Contact)

Figure 2.1. Load Types in CIRCLY

Since CIRCLY can model only circular loads, numerous circles are used to simulate the actual tire imprint. The contact stress data file for each combination of tire loading and tire inflation pressure has 12 or 13 columns and thousands of rows of non-zero data. To reduce the calculation

time, these data are simulated in CIRCLY by a number of circular loads with a diameter of 17 mm, which is equal to the center-to-center distance between adjacent instrumented pins in the SIM Mk IV system. In the 3-D stress model, the number of load columns is the same as the number of columns in the original data file, while the number of load rows is reduced to the round-off value of N calculated in Equation 2.1.

$$N = \frac{v}{d} \times \frac{N_r}{f} \tag{2.1}$$

in which:

N = number of load rows in the 3-D stress model;

v = tire speed in the test, mm/s;

N_r = number of rows with non-zero data in the original contact stress data file;

f = sampling frequency of the instrumented pins in the test, 1001 Hz; and

d = diameter of load circle in CIRCLY model, 17 mm.

In each column of the original data, a number (a rounded-off value of N_r / N) of rows of the data are summed up as one circular load in the modeled data. Figure 2.2 illustrates the 3-D stress model for Case L3P3 (shown in Table 2.1) with the target loading of 27.5 kN and the tire inflation pressure of 690 kPa. The load group in the 3-D stress model for Case L3P3 consists of 204 circles (12 columns by 17 rows) tangent to each other. Each circle is assigned specific values of the modeled data of vertical stress, longitudinal stress and transverse stress. Figure 2.3 compares the modeled data to the original data for Case L3P3. It can been seen from this figure that the two data sets in each stress component agree with each other, which indicates that the 3-D stress model is appropriate.

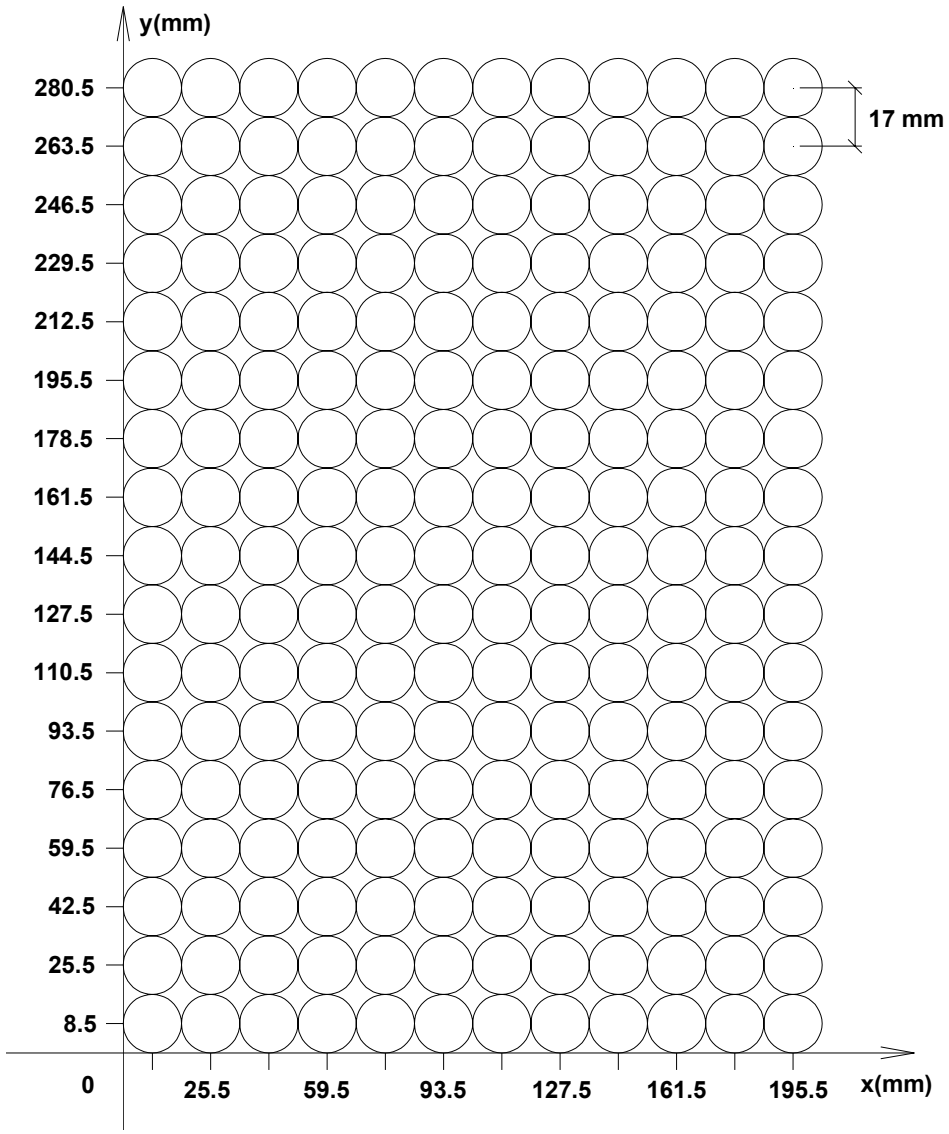

Figure 2.2. 3-D Non-Uniform Stress Model for Case L3P3 in CIRCLY

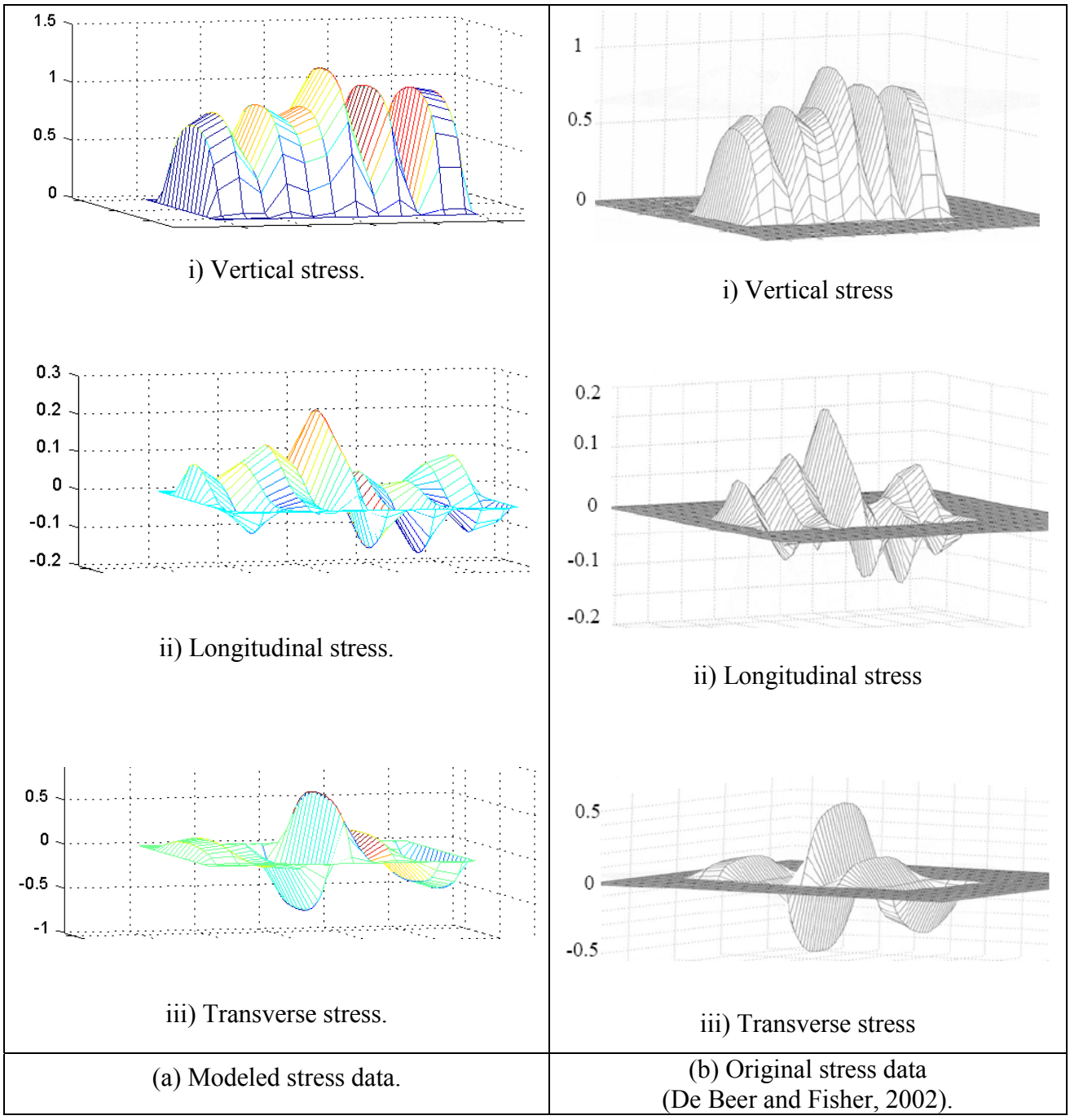

Figure 2.3. Comparisons of Modeled Stress Data with Original Stress Data for Case L3P3

The three prepared data sets (corresponding to the three stress components for the 3-D stress model) are inputted into CIRCLY to calculate pavement responses at three planes: i) pavement surface, ii) bottom of the asphalt layer, and iii) top of the subgrade. Pavement responses at the three planes will be used to estimate the top-down cracking, bottom-up cracking and pavement

rutting in the following chapters. During the calculation of pavement strains at the specified locations, the effects of all circular loads are superimposed in the data set of each stress component. The studied pavement area is larger than the contact area between tire and pavement for the purpose of analyzing the pavement responses under and adjacent to the contact area. The output file of CIRCLY includes three data sets of pavement response resulting from the three stress components separately. As a result, the effect of each stress component on pavement responses can be examined individually. In addition, the strains produced by the three stress components at each studied point are summed up to illustrate the resultant effect of the 3-D non-uniform stresses. Therefore, the individual effect of each stress component (vertical, longitudinal and transverse) will be estimated as well as the total effect of the three stress components. The following chapter will detail the pavement responses at the studied three planes.

Chapter 3 Evaluation of Pavement Reponses

3.1 Distributions of Pavement Strains under 3-D Stresses

The calculated pavement responses in a typical CIRCLY output file include stress, strain and displacement. Pavement strains are of special interest because the critical values of pavement strains are generally used to predict pavement performance. In this study, not only the critical strains but also the strain distributions are studied at each plane of pavement surface, asphalt bottom and subgrade top. At the pavement surface and the bottom of asphalt layer, the horizontal strains are analyzed including the longitudinal strain and transverse strain. It is important to note that longitudinal strains are responsible for transverse cracking, and transverse strains are accountable for longitudinal cracking. At the top of subgrade, the vertical strains are studied since they will be used to predict pavement rutting.

The distributions of all studied pavement strains are plotted using MATLAB for every one of the 7,500 cases in the experimental design. Each case has four pages of figures: i) strain distributions in pavement under the vertical stress; ii) strain distributions in pavement under the longitudinal stress; iii) strain distributions in pavement under the transverse stress; iv) strain distributions in pavement under the combined three stress components. Therefore, a total of 30,000 pages of figures have been generated in MATLAB and summarized in two DVDs which are available for free upon request. Appendix 1 provides information on how to obtain access to these 30,000 pages of figures. Each page has five or six figures displayed in three rows:

- First row: transverse strain distribution and longitudinal distribution at pavement surface;
- Second row: transverse strain distribution and longitudinal distribution at the bottom of asphalt layer;
- Third row: if the strain distributions correspond to a stress component, the vertical strain distribution at the top of subgrade and the corresponding stress component are graphically illustrated in the third row; if the strain distributions correspond to the combined 3-D stresses, only strain distribution at the top of subgrade is displayed in the third row.

For example, Figures 3.1 to 3.4 shows the strain distributions of Case L3P3, in which the asphalt thickness is 25 mm, asphalt modulus is 3,500 MPa, and the subgrade modulus is 75 MPa. Figure 3.1 consists of six sub-figures and illustrates pavement strain distributions under the vertical stress. The two sub-figures in the first row are longitudinal and transverse strain distributions at the pavement surface. The second row has two sub-figures presenting longitudinal and transverse strain distributions at the bottom of the asphalt layer. The third row also has two sub-figures: the left one is the vertical strain distribution at the top of pavement subgrade; the right one is the vertical contact stress applied to the pavement surface. Below the six sub-figures in Figure 3.1 is a short note that explains the values of variables in this case: L represents the tire loading; P represents the tire inflation pressure; H_a is the thickness of the asphalt layer; E_a symbolizes the asphalt modulus; and E_s is the modulus of subgrade. Figure 3.2 illustrates the strain distributions in the pavement under longitudinal stress; Figure 3.3 shows the strain distributions in the pavement under transverse stress; and Figure 3.4 presents the strain distributions in the pavement under the combined 3-D stress.

Horizontal strains at pavement surface are analyzed because they are directly related to top-down cracks. By considering the three stress components separately, for all the pavement structures, the vertical contact stress produces compressive horizontal strains in the tire-pavement contact area and tensile horizontal strains around the contact area at the pavement surface. The transverse contact stress produces tensile longitudinal strains not only outside the contact area but also in the contact area, which partially reduces the compressive strains resulting from the vertical contact stress. The transverse contact stress does not show a significant effect on the transverse strains at pavement surface. The longitudinal stress has marginal effect on either longitudinal strain or transverse strain. As a result, only vertical stress and transverse stress show considerable effects on the longitudinal strain at the pavement surface. The vertical stress controls the transverse strain at the pavement surface. As the asphalt thickness and modulus increase, the effect of every stress component decreases on both longitudinal and transverse strains at the surface of the asphalt layer. The subgrade modulus does not show appreciable effect on the pavement strains at the asphalt surface.

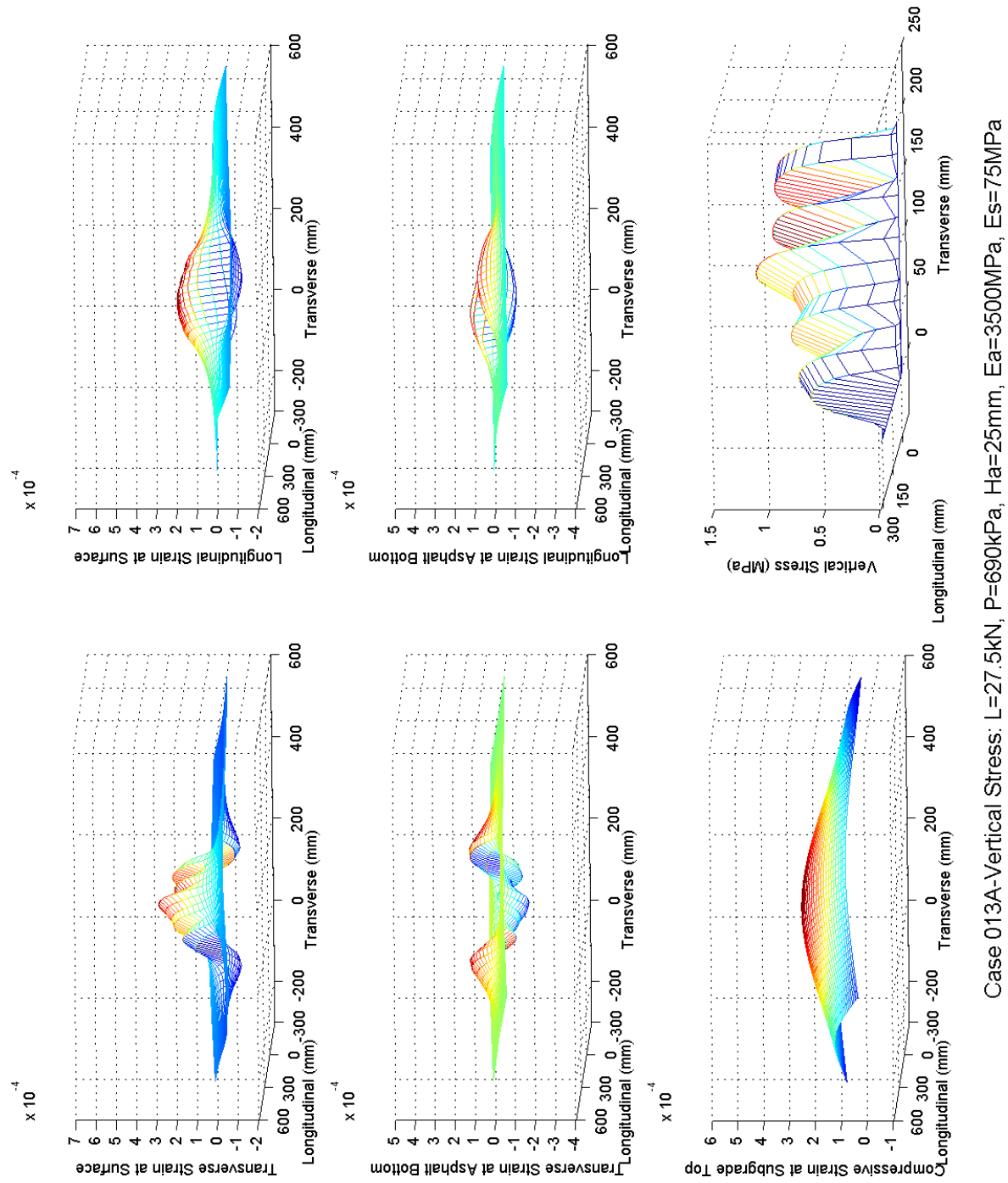

Figure 3.1. Pavement Strain Distributions under Vertical Stress for Case L3P3

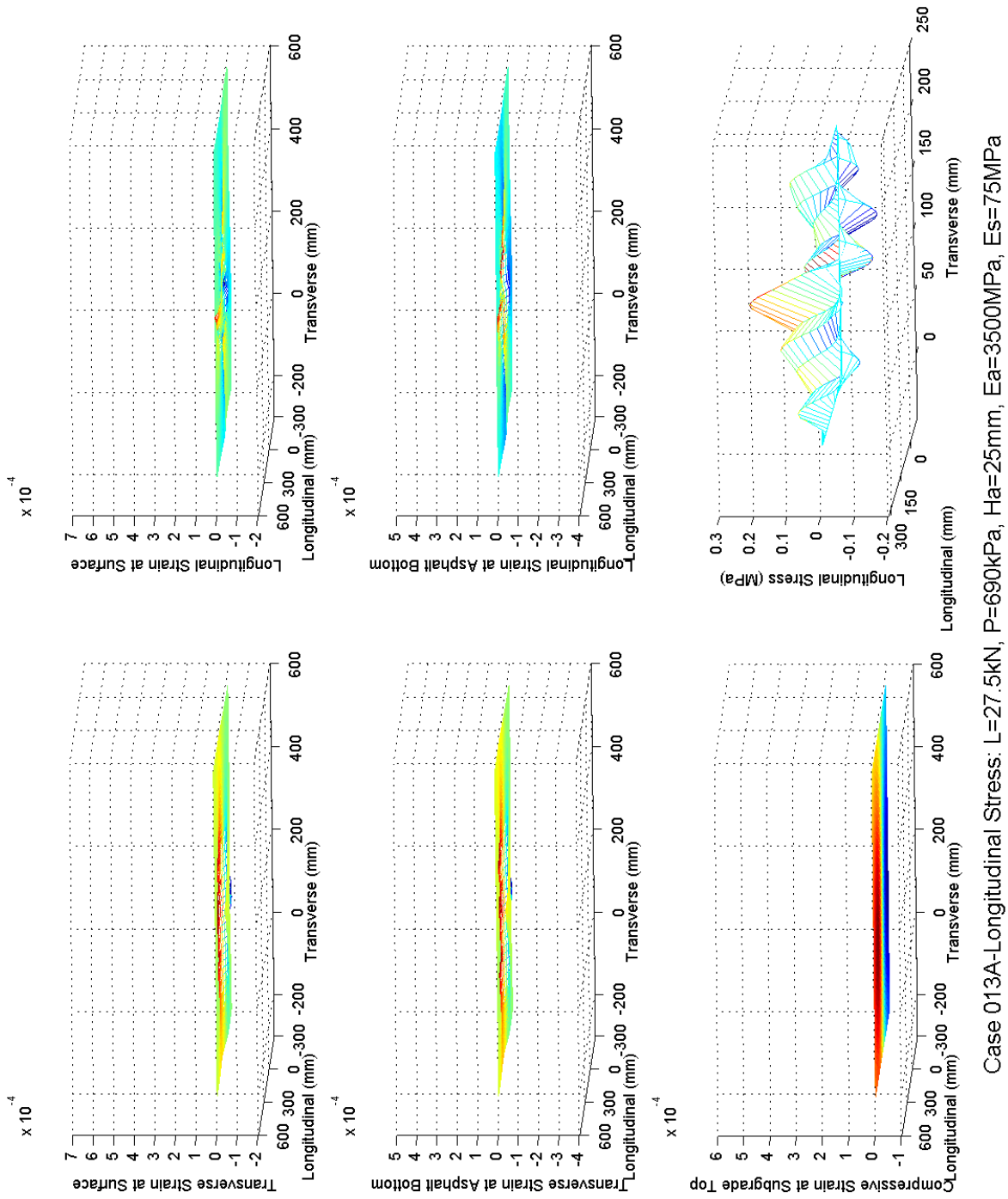

Figure 3.2. Pavement Strain Distributions under Longitudinal Stress for Case L3P3

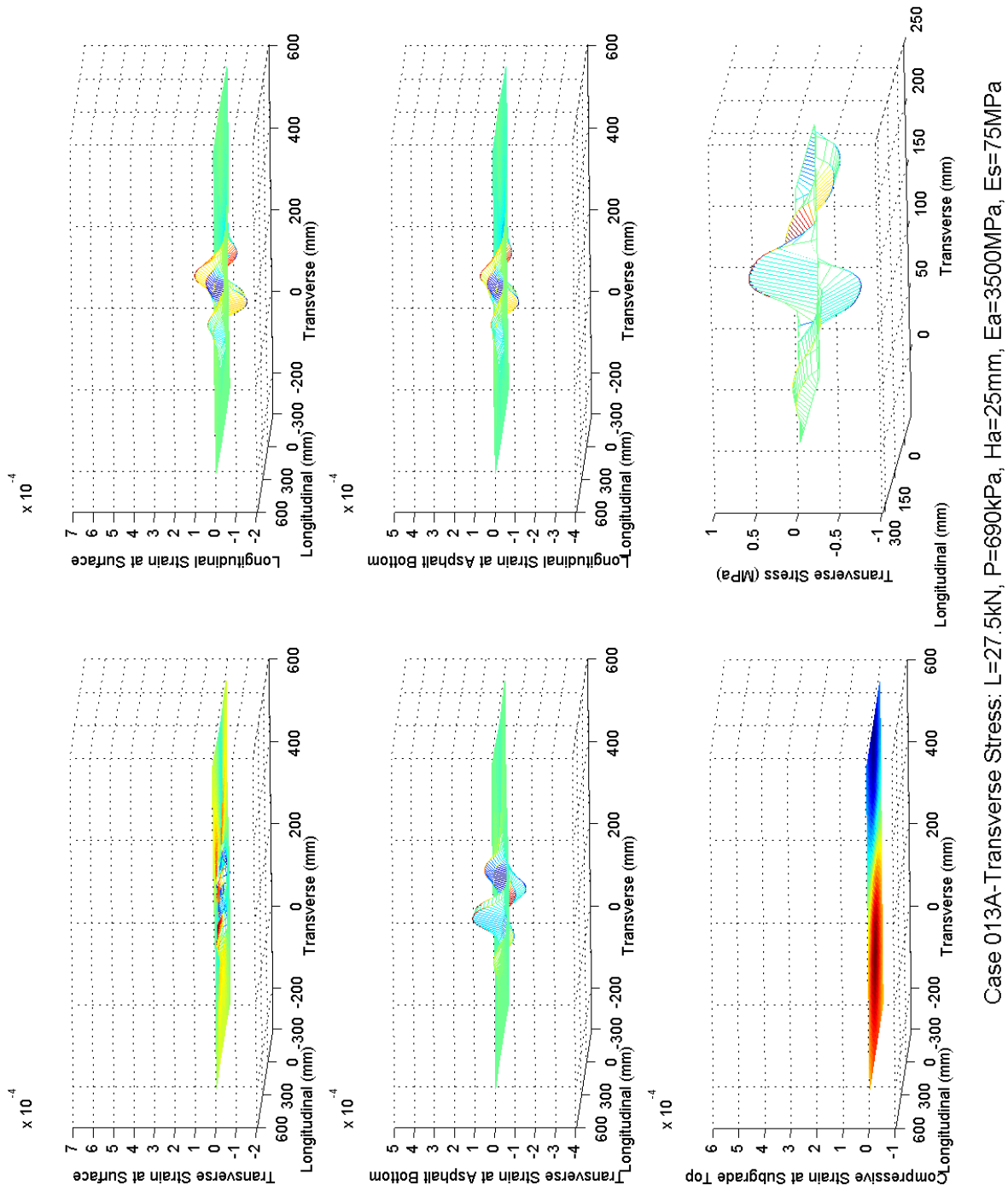

Figure 3.3. Pavement Strain Distributions under Transverse Stress for Case L3P3

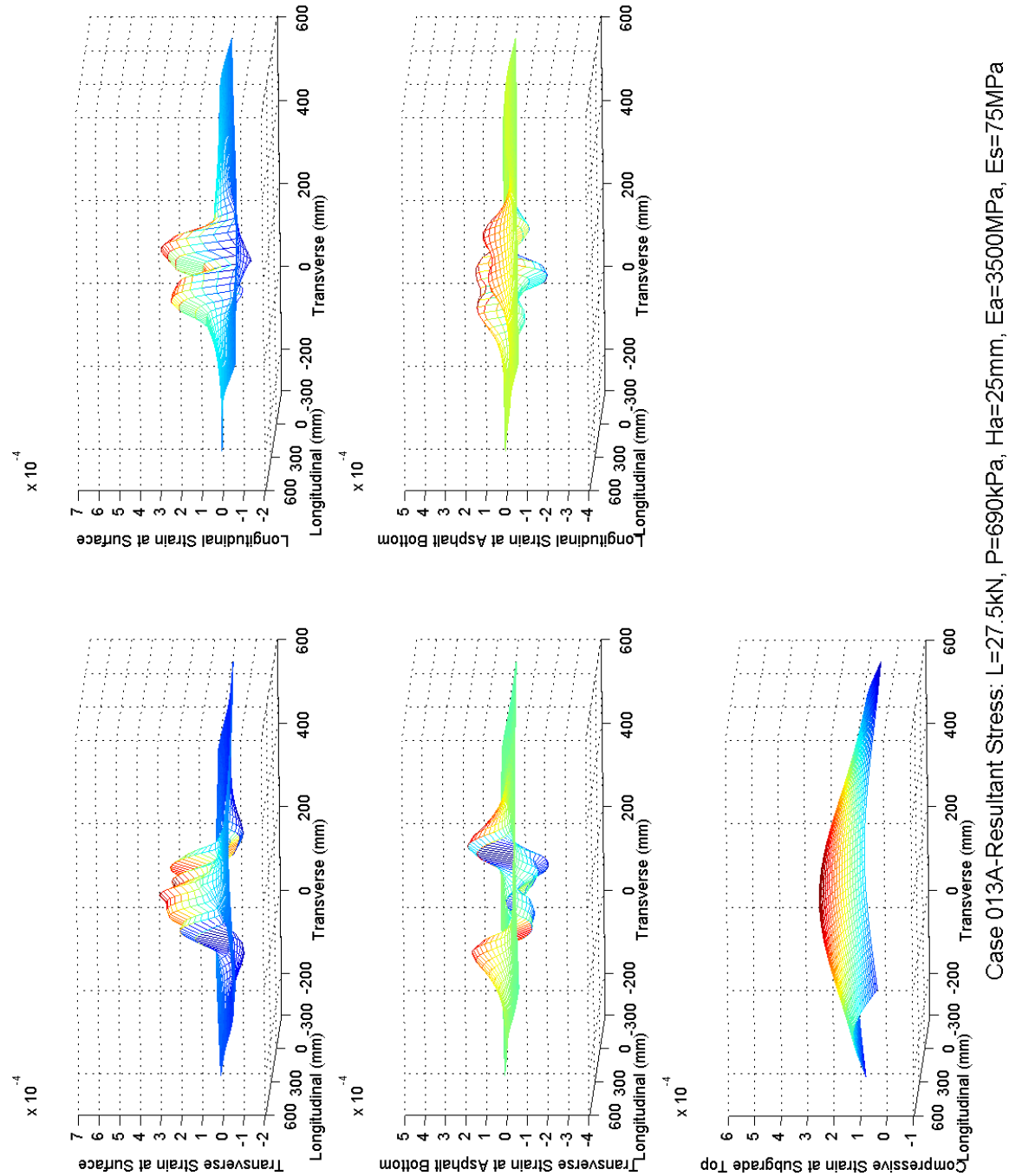

Figure 3.4. Pavement Strain Distributions under 3-D Stress for Case L3P3

Horizontal strains at the bottom of the asphalt layer are of special interest since they are used to predict bottom-up pavement cracks. When comparing the strain distributions in every case, it can be found that the vertical stress has the dominant effect on horizontal strains at the bottom of the asphalt layer. Because of tire tread, the measured vertical stress shows several peak stresses (see Figure 2.3). This is reflected in pavements with a thin asphalt layer but not in thick-asphalt pavements. The applied transverse stress has a significant effect on horizontal strains at asphalt bottom only in a pavement with a thin asphalt layer. As the asphalt thickness and modulus increase, the effect of the transverse stress decreases. Of all the three stress components, longitudinal stress shows the least effect on the strains at the bottom of the asphalt layer, and its effect also decreases as the asphalt thickness and modulus increase. The subgrade modulus does not show noticeable influence on the horizontal strains at the asphalt bottom. Under the combined 3-D stresses, when the asphalt layer is relatively thin, two peak tensile strains appear within the contact area at the plane of the asphalt bottom, while compressive strains show in the edge and outside of the contact area. For pavements with the thinnest asphalt layer (25 mm), the compressive strain appears around the center of the contact area. The shape of the transverse strain distribution can be referred to as "w-shape" for the pavements with a thin asphalt layer. As the asphalt thickness and modulus increases, the transverse strain distribution changes from a "w-shape" to a "u-shape".

Vertical strains at the top of pavement subgrade are studied because they are generally used to predict rutting at pavement surface. Subgrade modulus considerably affects the magnitude of vertical strain at the top of subgrade. The increase of subgrade modulus decreases the vertical compressive strain at the subgrade top. The increase of asphalt modulus also decreases the vertical strain at the subgrade top.

3.2 Strain Distributions under Uniform Stress

In the 3-D stress model proposed in the previous chapter, the measured non-uniform tire-pavement contact stresses in three directions are applied over the measured non-circular contact area. In contrast, for most pavement design methods, the tire-pavement contact area is assumed to be a circle and is loaded with uniform vertical stress equal to the tire inflation pressure. The

radius of the circular contact area is calculated using the tire load and tire inflation pressure. For instance, if the measure load is 26.3 kN and the tire inflation pressure is 690 kPa, the radius of the circle will be 110 mm. Figure 3.5 illustrates the uniform stress model of Case L3P3. Because of the assumptions in loading conditions that are different from the actual situation, the uniform stress model may lead to potential errors in predicting the pavement responses. To address the possible errors caused by the uniform stress model, the 3-D stress model is compared with the uniform stress model by means of the distributions and critical values of pavement strains.

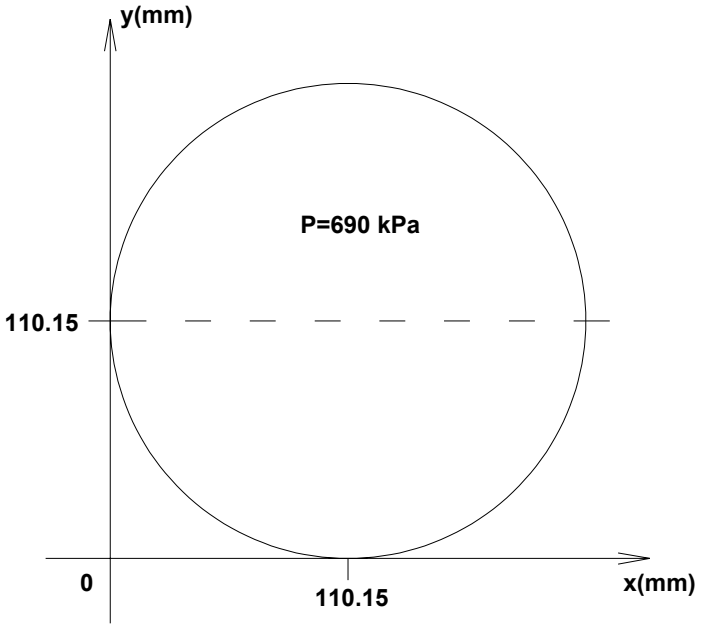

Figure 3.5. Uniform Vertical Stress Model for Case L3P3 in CIRCLY

The horizontal strains at the pavement surface and at asphalt bottom, and the vertical strain at subgrade top, are evaluated by the uniform stress model using CIRCLY within the same area studied in the 3-D stress model. Because of symmetry, the longitudinal strain and transverse strain at every plane in the pavement have exactly the same distributions and critical values at all levels of asphalt thickness, asphalt modulus, subgrade modulus, tire load and tire inflation pressure. Figure 3.6 shows the strains in a pavement under a tire load of 26.3 kN and tire inflation pressure of 690 kPa when the asphalt thickness is 25 mm, asphalt modulus is 3,500 MPa, and subgrade modulus is 75 MPa. Figure 3.6 has the same layout as Figure 3.4: the two figures in the first row are transverse strain distribution and longitudinal strain distribution at

pavement surface; the second row includes the figures of transverse strain distribution and longitudinal strain distribution at the bottom of the asphalt layer; the figure in the third row is the vertical strain distribution at the top of subgrade.

Compared to the strain distributions resulting from the 3-D non-uniform stresses in Figure 3.4, each strain distribution produced by the uniform stress model has a symmetric shape. For pavements with a thin asphalt layer, the uniform stress model results in higher tensile strains in a larger area at the pavement surface than the 3-D stress model. As the asphalt thickness and modulus increase, the magnitude of tensile strains at pavement surface tends to decrease, which is similar to the cases with 3-D stresses. For pavements with a thicker asphalt layer, the difference in the horizontal strain distributions at pavement surface is less significant between the 3-D stress model and the uniform stress model.

When the pavement is subjected to uniform stress, the horizontal strain distributions at the bottom of the asphalt layer have a "u-shape" if the pavement has a thin asphalt layer. With the increase of the asphalt layer, the "u-shape" strain distribution tends to have a "v-shape", and the magnitude of the overall strains increases initially and then decreases. The "u-shape" is the result of the effect of the tire confinement on the development of strains at the bottom of the asphalt. As the thickness increases, it can be observed that the strains fully develop a peak ("v-shape").

The strain distributions at the top of the subgrade resulting from the uniform stress are not significantly different from the 3-D non-uniform stresses. The shape of the strain distribution and the magnitude of the strains at the subgrade top are almost the same between the uniform stress case and the 3-D uniform stress case. This finding indicates that the shape and distribution of the tire-pavement contact stress has more effect on the strains in the upper layer of the pavement, such as the asphalt layer, but little effect on the strains in the lower layer (subgrade). In other words, with the same wheel load and tire inflation pressure, the uniform stress model and 3-D stress model produce approximately the same vertical strain at subgrade top. Therefore, the assumptions on the tire-pavement contact conditions in most traditional pavement design methods are reasonable to estimate the vertical strain at the top of pavement subgrade.

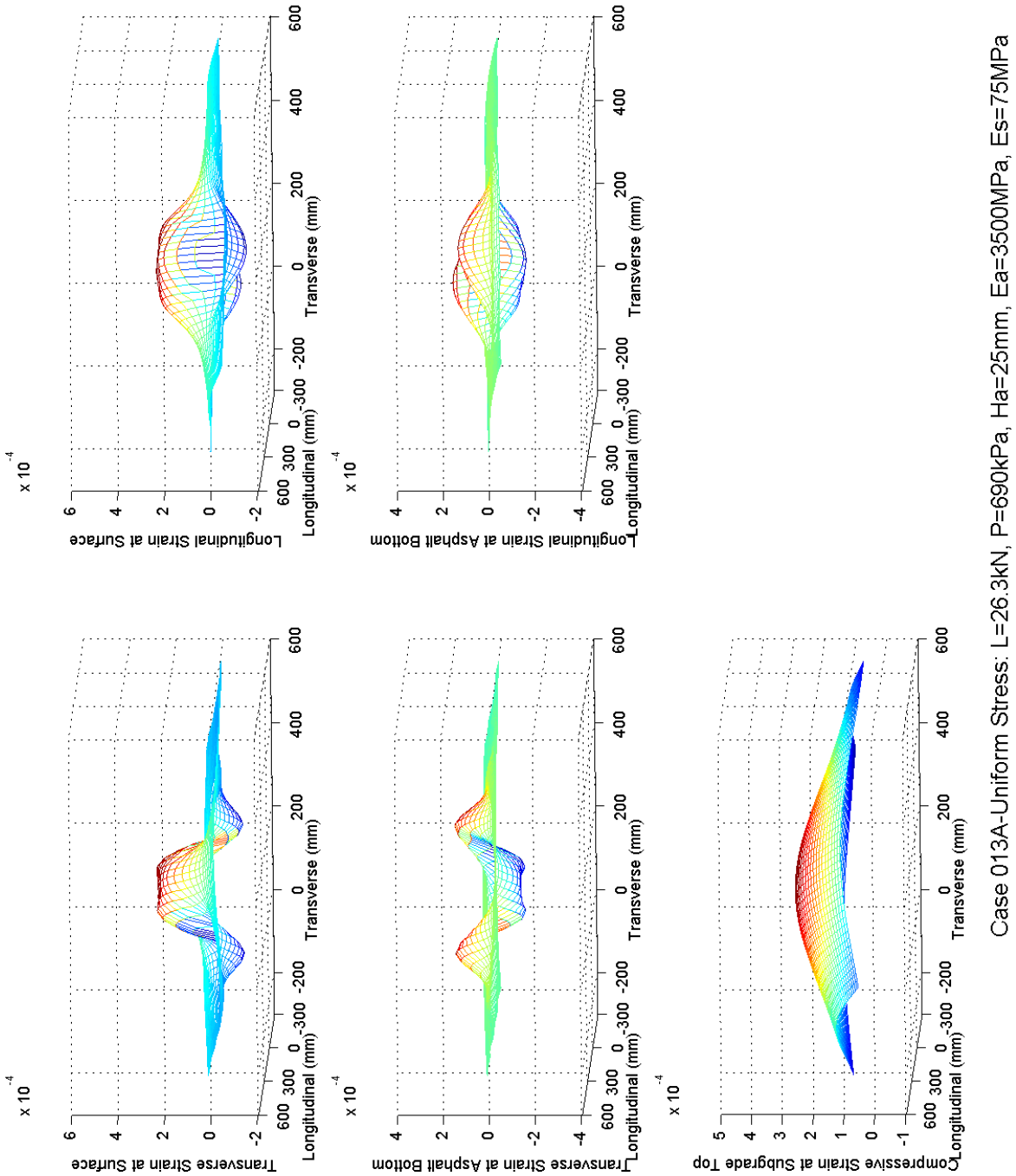

Figure 3.6. Pavement Strain Distributions under Uniform Stress for Case L3P3

3.3 Comparison of Critical Strains

The critical strains of the 3-D stress model and uniform stress model are compared by studying the difference of the critical strains calculated in the two models. "Critical strain" in this research means the maximum value of tensile strains at the pavement surface or the asphalt bottom in either longitudinal direction or transverse direction, or the maximum value of the vertical strains at the top of the subgrade. When calculating the difference of the critical strains, the absolute values of the studied strains are used for convenience. The absolute values are calculated by Equation 3.1, in which a positive value of D_ε indicates that the magnitude of the critical strain predicted by the 3-D stress model is higher than that predicted by the uniform stress model, and vice versa.

$$D_\varepsilon = |\varepsilon_n| - |\varepsilon_u| \tag{3.1}$$

where:

D_ε = difference of the critical strains calculated in the two models;

ε_n = critical strain calculated in the 3-D non-uniform stress model; and

ε_u = critical tensile strain calculated in the uniform stress model.

A number of figures are plotted in order to illustrate the effects of different variables on D_ε. These figures are presented in three groups in this chapter:

- Group A: Figures 3.7 to 3.11, showing the effect of asphalt modulus, in Section 3.3.1;
- Group B: Figures 3.12 to 3.16, presenting the effect of subgrade modulus, in Section 3.3.2; and
- Group C: Figures 3.17 to 3.21, illustrating the combined effect of tire load and tire inflation pressure, in Section 3.3.3.

In each group, there are five figures:

- Difference of critical transverse tensile strains at pavement surface predicted by 3-D stress model and uniform stress model;
- Difference of critical longitudinal tensile strains at pavement surface predicted by 3-D stress model and uniform stress model;

- Difference of critical transverse tensile strains at asphalt bottom predicted by 3-D stress model and uniform stress model;
- Difference of critical longitudinal tensile strains at asphalt bottom predicted by 3-D stress model and uniform stress model; and
- Difference of critical vertical strains at subgrade top predicted by 3-D stress model and uniform stress model.

The capital letters, A, B and C, are attached to the end of the figures to differentiate the figures with the same caption but in different groups. For example, Figure 3.7 has a capital letter A at the end of its caption, which indicates that this figure is in Group A showing the effect of asphalt modulus. In similar fashion, Figure 3.12 has a capital letter B at the end of the caption in order to show that this figure is in Group B showing the effect of subgrade modulus.

3.3.1 Effect of Asphalt Modulus and Asphalt Thickness

Figures 3.7 to 3.11 (Group A) show the effect of asphalt modulus on the critical strains at the asphalt top, the bottom of the asphalt layer, and the top of the subgrade layer. In the five figures, the other three variables, tire load, tire pressure and subgrade modulus, are at constant levels so that the effects of asphalt modulus and asphalt thickness are clear in the illustrations.

Figure 3.7 shows that, for a pavement with a thin asphalt layer (≤ 70 mm), the critical tensile strains at pavement surface calculated by the 3-D stress model are smaller than those predicted by the uniform stress model regardless of the magnitude of the asphalt modulus. When the asphalt thickness is less than 70 mm, a higher asphalt modulus is associated with a smaller difference in the critical transverse tensile strains at the pavement surface predicted by the two models. When the asphalt layer is thicker than 70 mm, most D_ε s in the transverse direction at the pavement surface are within 10 micros, which indicates that the two models produce similar results in this situation. The only exception is the case with a low asphalt modulus (L3P3-1500-75), which has a relatively large D_ε when the asphalt is thicker than 160 mm but the magnitude of D_ε is still less than 15 micros. Figure 3.7 indicates that the traditional uniform stress model overestimates the transverse tensile strain at the surface of a pavement with a thin asphalt layer.

If the asphalt layer is thicker than 70 mm, the uniform stress model is more reliable for predicting the surface tensile strain in the transverse direction that is perpendicular to the vehicle travel direction.

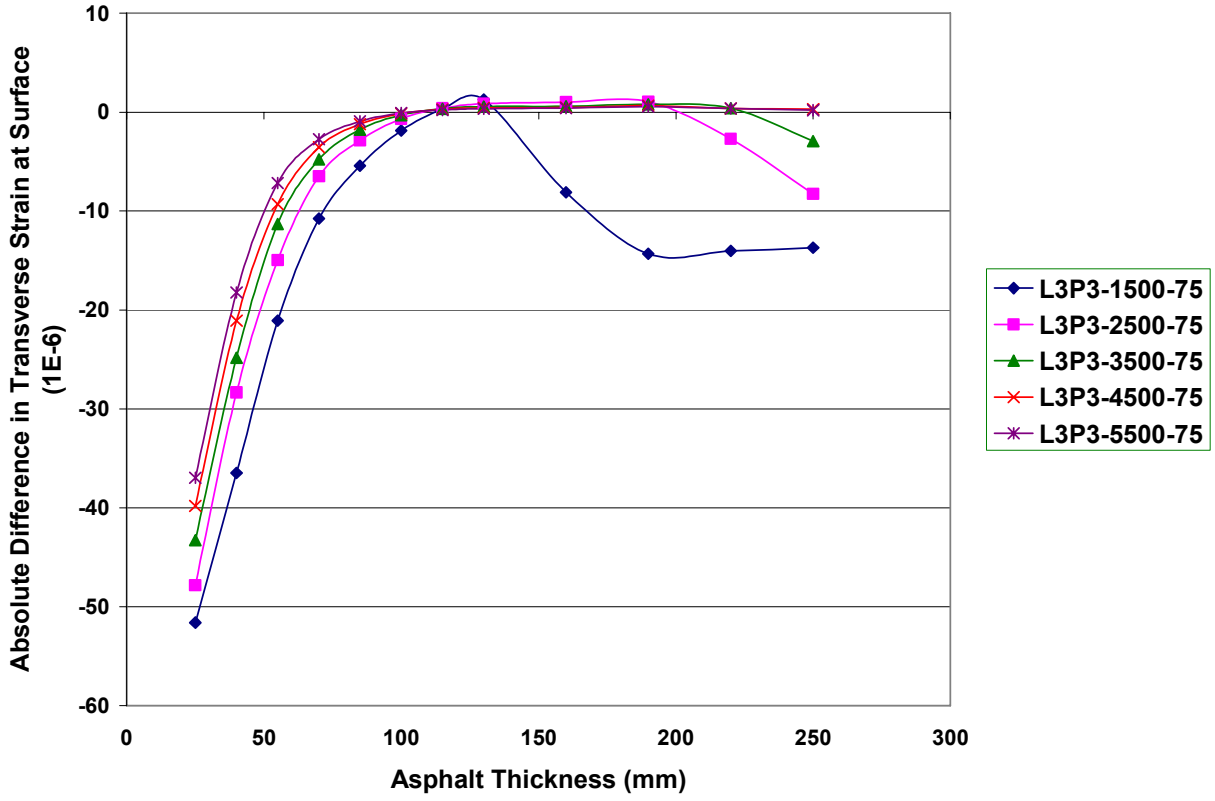

Figure 3.7. Differences in Critical Transverse Tensile Strains at Pavement Surface Predicted by 3-D Stress Model and Uniform Stress Model (A)

Figure 3.8 presents the differences in the critical longitudinal tensile strains at the pavement surface calculated by the 3-D stress model and the uniform stress model. When the asphalt modulus is at a low level (1,500 MPa), the critical strains predicted by the 3-D stress model are larger than those calculated by the uniform stress model. As the asphalt modulus increases, D_ε decreases and some values of D_ε become negative when the asphalt is relatively thin. The magnitudes of D_ε are within ±10 micros when the asphalt thickness is between 55 mm and 190 mm and when the asphalt modulus is not less than 3500 MPa. In other words, when the modulus and thickness of the asphalt layer are within specific ranges, the uniform stress model produces

critical longitudinal tensile strains at the pavement surface that are similar to those of the 3-D non-uniform stress model.

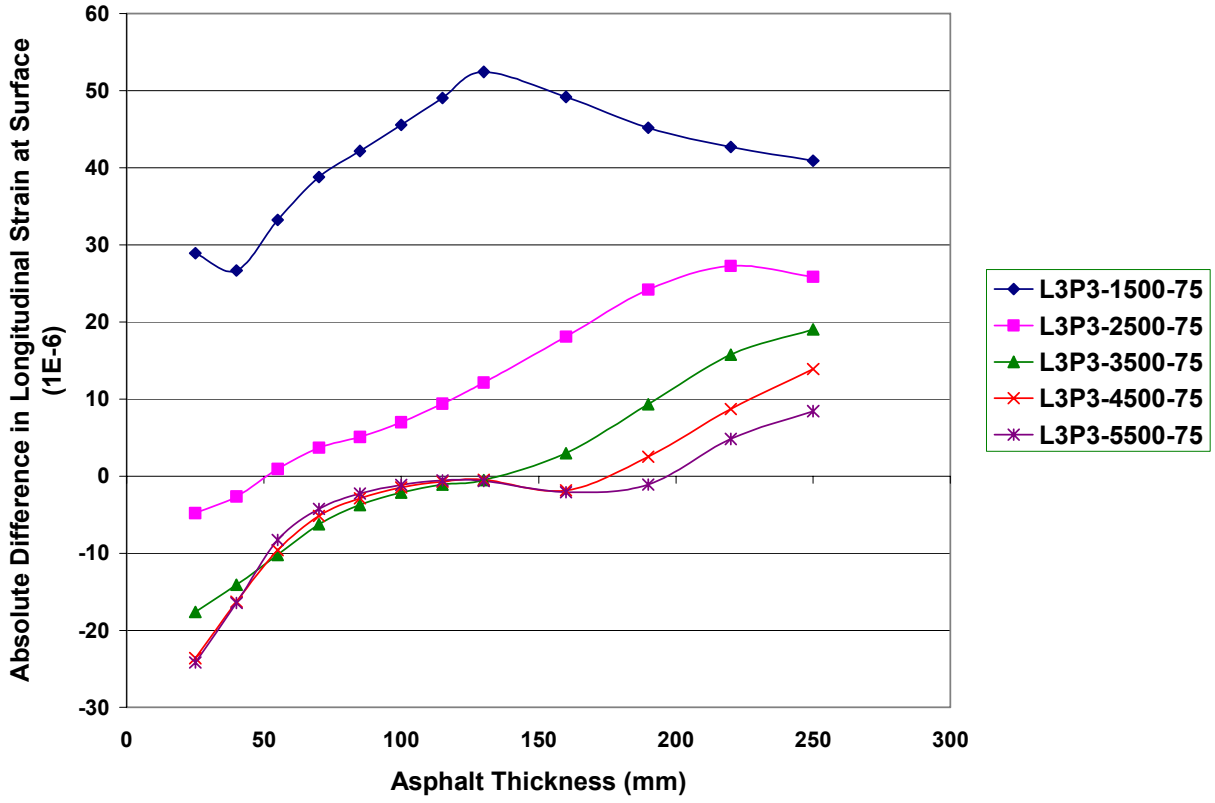

Figure 3.8. Differences in Critical Longitudinal Tensile Strains at Pavement Surface Predicted by 3-D Stress Model and Uniform Stress Model (A)

Figure 3.9 illustrates the differences in the critical transverse tensile strains at the bottom of the asphalt layer predicted by the uniform stress model and the 3-D stress model. The uniform stress model underestimates the transverse tensile strains at the asphalt bottom when the asphalt layer is thin, and overestimates the transverse tensile strains at the asphalt bottom when the asphalt layer is between 70 mm and 130 mm regardless of the asphalt modulus. When the asphalt modulus is very small, i.e. 1,500 MPa, the absolute values of D_ε are large (up to 117 micros) when the asphalt thickness is less than 160 mm. As the asphalt modulus increases, the absolute values of D_ε tend to decrease, which indicates that the uniform stress model becomes more reliable to calculate the transverse tensile strains at the bottom of the asphalt layer with a larger modulus. When the asphalt thickness is no less than 160 mm, the uniform stress model and the 3-D stress

model produce similar critical transverse tensile strains at the asphalt bottom regardless of the asphalt modulus.

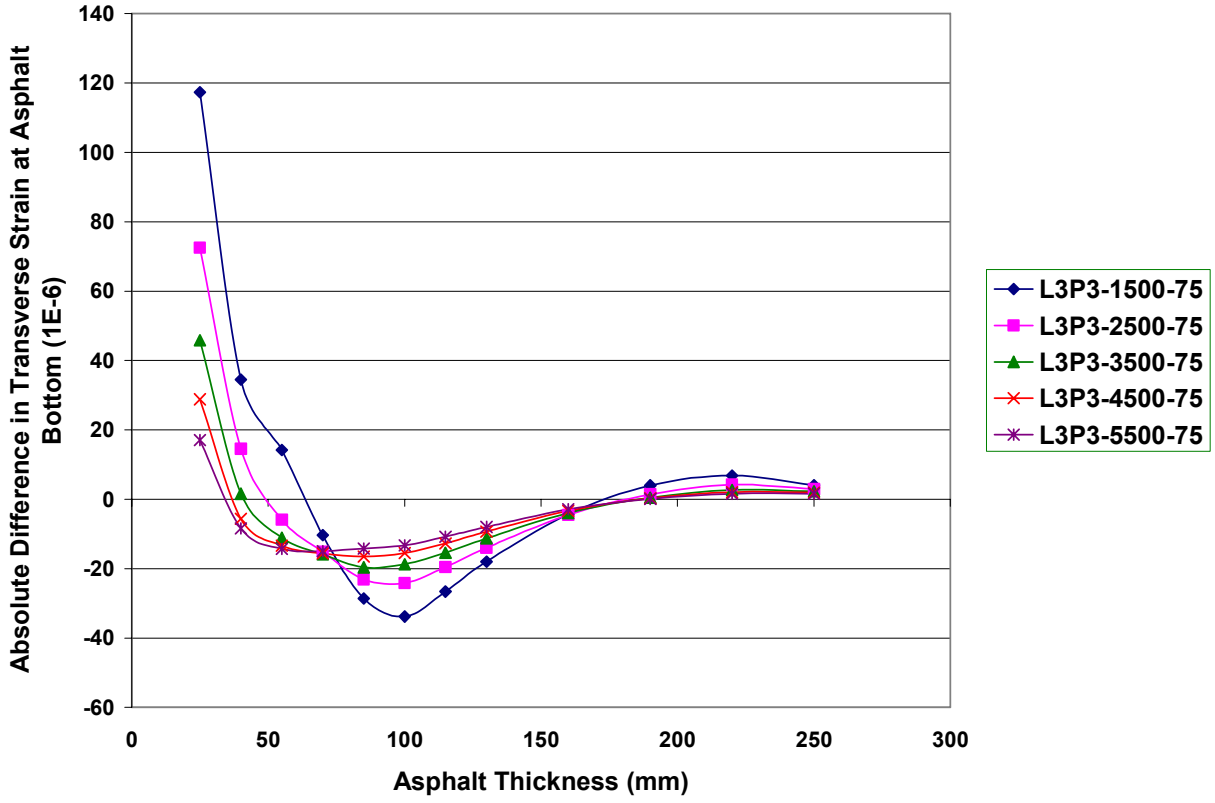

Figure 3.9. Differences in Critical Transverse Tensile Strains at Asphalt Bottom Predicted by 3-D Stress Model and Uniform Stress Model (A)

Figure 3.10 displays the values of D_ε in the critical longitudinal tensile strains at the asphalt bottom calculated by the two models. The trends in Figure 3.10 are similar to those in Figure 3.9: when the asphalt layer is not thicker than 40 mm, the uniform stress model underestimates the critical longitudinal tensile strains at the asphalt bottom at all asphalt modulus levels; when the asphalt thickness is between 85 mm and 130 mm, the uniform stress model overestimates the critical longitudinal strains at asphalt bottom regardless of the asphalt modulus; and when the asphalt thickness is no less than 160 mm, the two models produce similar results. A lower asphalt modulus is associated with a larger absolute value of D_ε when the asphalt layer is less than 160 mm.

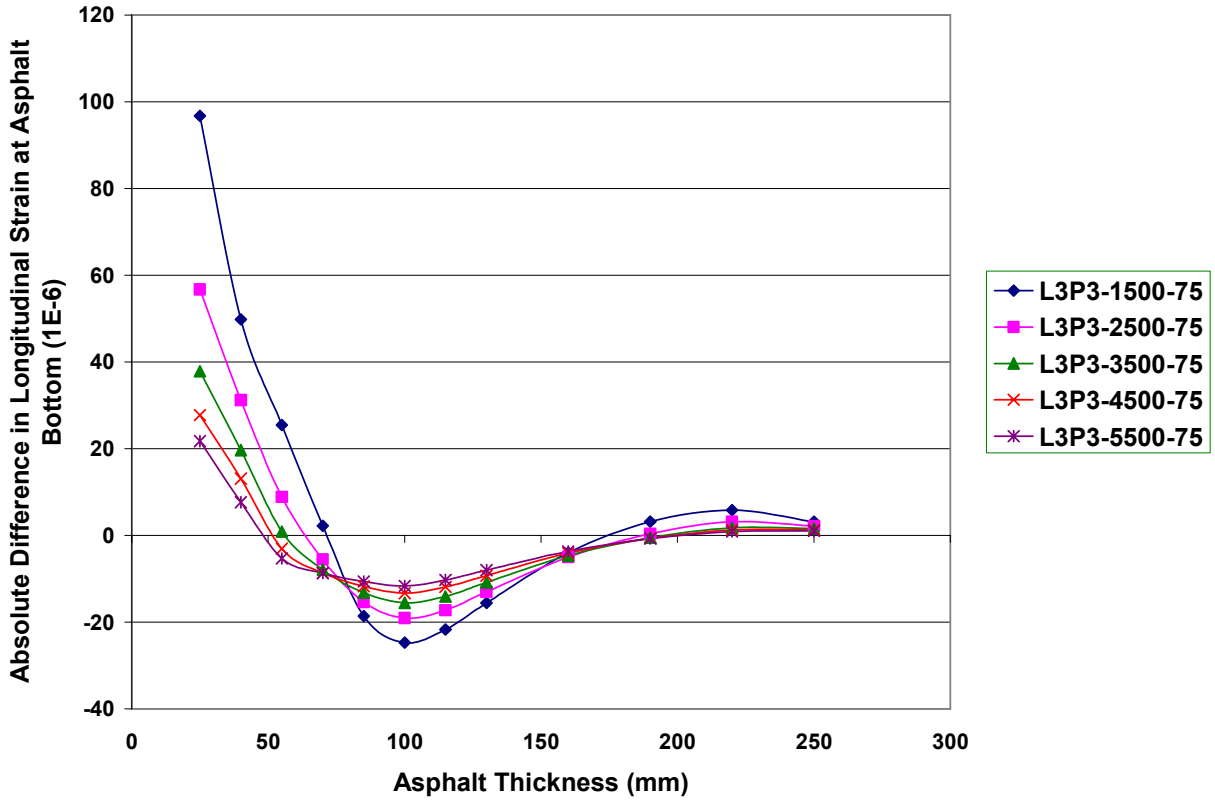

Figure 3.10. Differences in Critical Longitudinal Tensile Strains at Asphalt Bottom Predicted by 3-D Stress Model and Uniform Stress Model (A)

The asphalt modulus does not show significant effect on D_ε in the critical vertical strains at the top of subgrade, as shown in Figure 3.11. The absolute values of D_ε are within 2 micros at all asphalt modulus levels and all asphalt thickness levels. Figure 3.11 indicates that the uniform stress model and the 3-D stress model produce almost the same vertical strains at the subgrade top. This figure also shows that D_ε in the critical vertical strains at subgrade top is almost independent of the thickness and modulus of the asphalt layer.

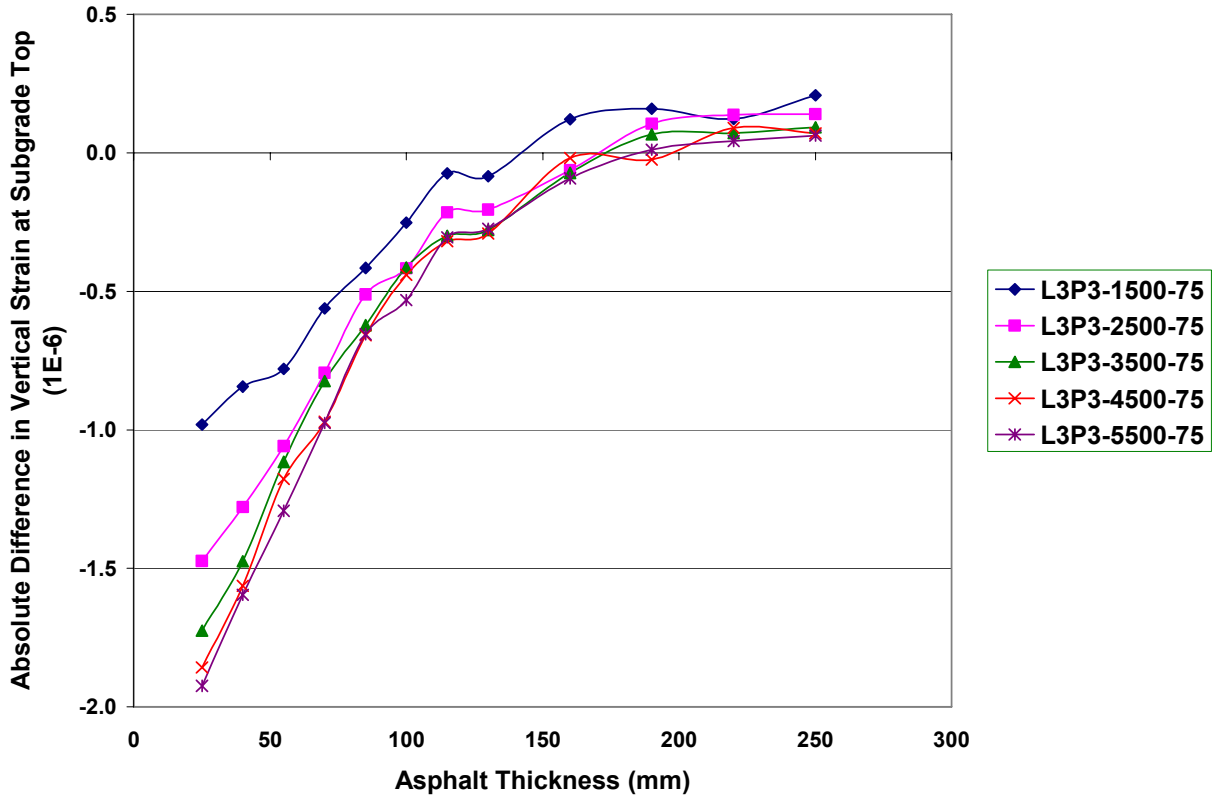

Figure 3.11. Differences in Critical Vertical Strains at Subgrade Top Predicted by 3-D Stress Model and Uniform Stress Model (A)

In summary, Figures 3.7 to 3.11 show that the modulus and thickness of the asphalt layer have significant effects on D_ε in horizontal tensile strains (both transverse strains and longitudinal strains) in the asphalt layer (at asphalt surface and at asphalt bottom) but not on D_ε in vertical strains at the subgrade top. A low asphalt modulus and a small asphalt thickness are associated with a larger absolute value of D_ε in the horizontal tensile strains in the asphalt layer. With a higher asphalt modulus and larger asphalt thickness, the uniform stress model and the 3-D stress model tend to produce closer strains in the asphalt layer.

3.3.2 Effects of Subgrade Modulus and Asphalt Thickness

As stated in the previous sections, five levels of subgrade modulus are considered in the experimental design. The effect of subgrade modulus on the studied pavement strains is illustrated in Group B: Figures 12 to 16, every one of which has a capital letter B at the end of the caption in order to indicate the figure is in Group B. In each of the five figures, three

variables are at constant levels: tire load, tire inflation pressure and asphalt modulus. Therefore, the effects of subgrade modulus and asphalt thickness on the difference in critical strains predicted by the 3-D stress model and uniform stress model are more clearly seen.

Figures 3.12 through 3.16 share a common characteristic: subgrade modulus does not show a significant effect on D_ε in critical strains predicted by the two models. When the subgrade modulus changes from 25 MPa to 125 MPa, D_ε in horizontal strains at pavement surface varies in a range of 7 micros according to Figures 3.12 and 3.13. The change of D_ε in horizontal strains at asphalt bottom with the variation of subgrade modulus is not appreciable in Figures 3.14 and 3.15. As shown in Figure 3.16, D_ε in vertical strain at subgrade top is within ±2.5 micros, and D_ε varies in a range of 1 micro with the change of subgrade modulus. As a result, the uniform stress model produces similar critical strains to the 3-D stress model when only subgrade modulus varies.

The effect of asphalt thickness is significant on the magnitude of D_ε in critical strains at pavement surface and at asphalt bottom, but not at the subgrade top. At the pavement surface, D_ε in transverse strains has negative values when the asphalt thickness is less than 100 mm. As the asphalt layer becomes thicker, the absolute values of D_ε decrease. When the asphalt layer is thicker than 55 mm, the absolute values of D_ε are less than 10 micros. Figure 3.12 indicates that the uniform stress model overestimates the transverse strain at the surface of a pavement with a thin asphalt layer. When the asphalt thickness increases, the uniform stress model and the 3-D stress model tend to produce similar transverse strains at pavement surface. In Figure 3.13, values of D_ε are around -18 when the asphalt thickness is 25 mm; as the asphalt thickness increases, D_ε increases to approximately 0 when the asphalt thickness reaches 130 mm; when the asphalt layer is thicker than 130 mm, D_ε becomes positive and continues to increase to around 19 when the asphalt is 250 mm. Figure 3.13 implies that the uniform stress model overestimates the critical longitudinal strains at the pavement surface when the asphalt layer is relatively thin, but underestimates the critical longitudinal strains when the asphalt layer is thicker than 130 mm.

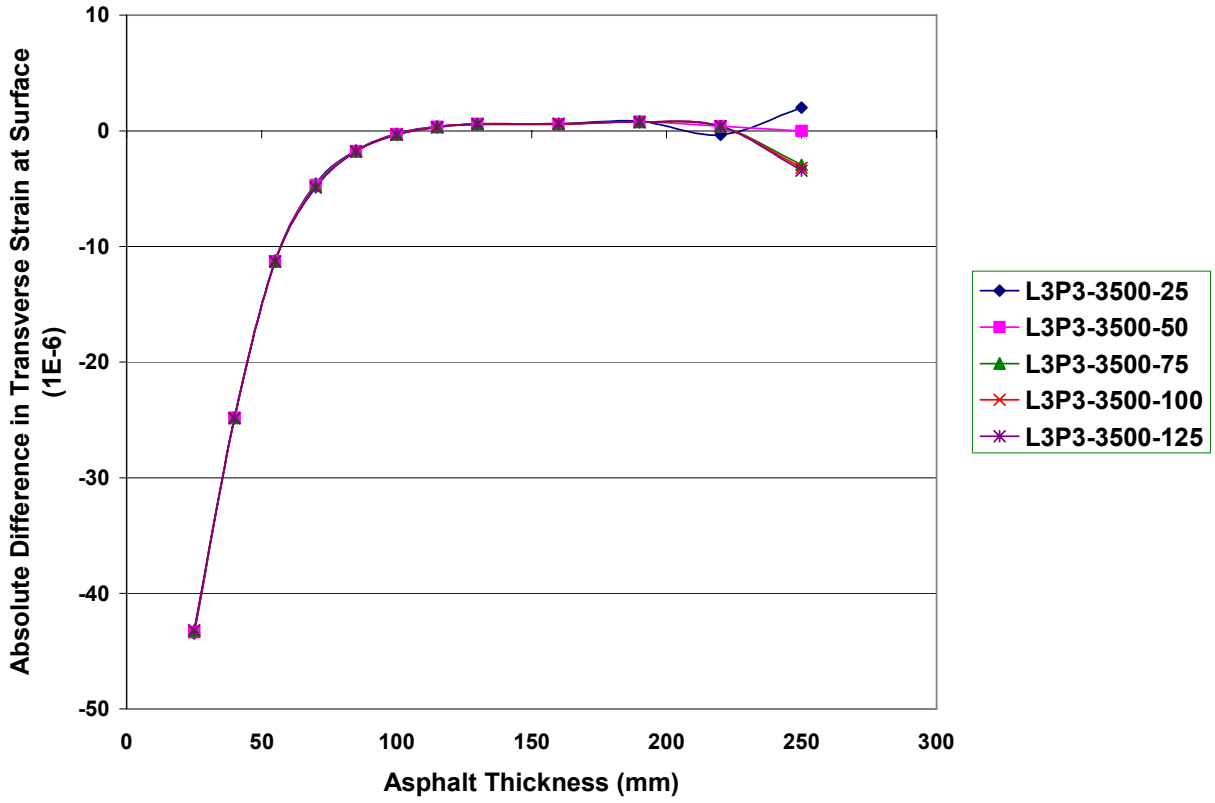

Figure 3.12. Differences in Critical Transverse Tensile Strains at Pavement Surface Predicted by 3-D Stress Model and Uniform Stress Model (B)

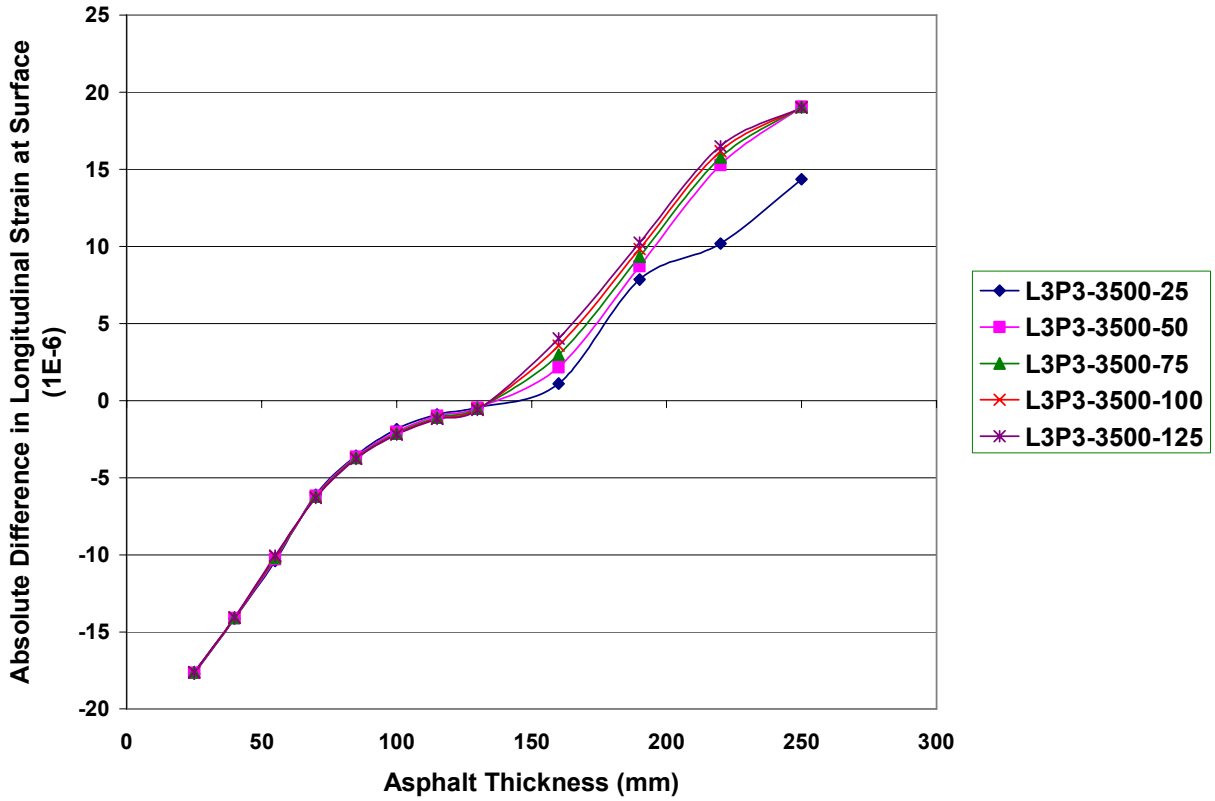

Figure 3.13. Differences in Critical Longitudinal Tensile Strains at Pavement Surface Predicted by 3-D Stress Model and Uniform Stress Model (B)

As shown in Figure 3.14, at the bottom of the asphalt layer, D_ε in transverse strains has positive values when the asphalt layer is 25 mm. The magnitude of D_ε in transverse strains is close to zero when the asphalt thickness is 40 mm. When the asphalt thickness increases from 40 mm to 130 mm, D_ε in transverse strains decreases from zero to around -20 micros, and then increases to approximately -10 micros. When the asphalt is thicker than 130 mm, the magnitude of D_ε in transverse strains varies in a range of ±10 micros. Figure 3.14 indicates that the uniform stress model underestimates the transverse strains at pavement surface when the asphalt layer is very thin, overestimates the transverse strains at pavement surface when the asphalt thickness is between 55 mm and 130 mm, and produces similar results to the 3-D stress model when the asphalt thickness is around 40 mm and is larger than 160 mm.

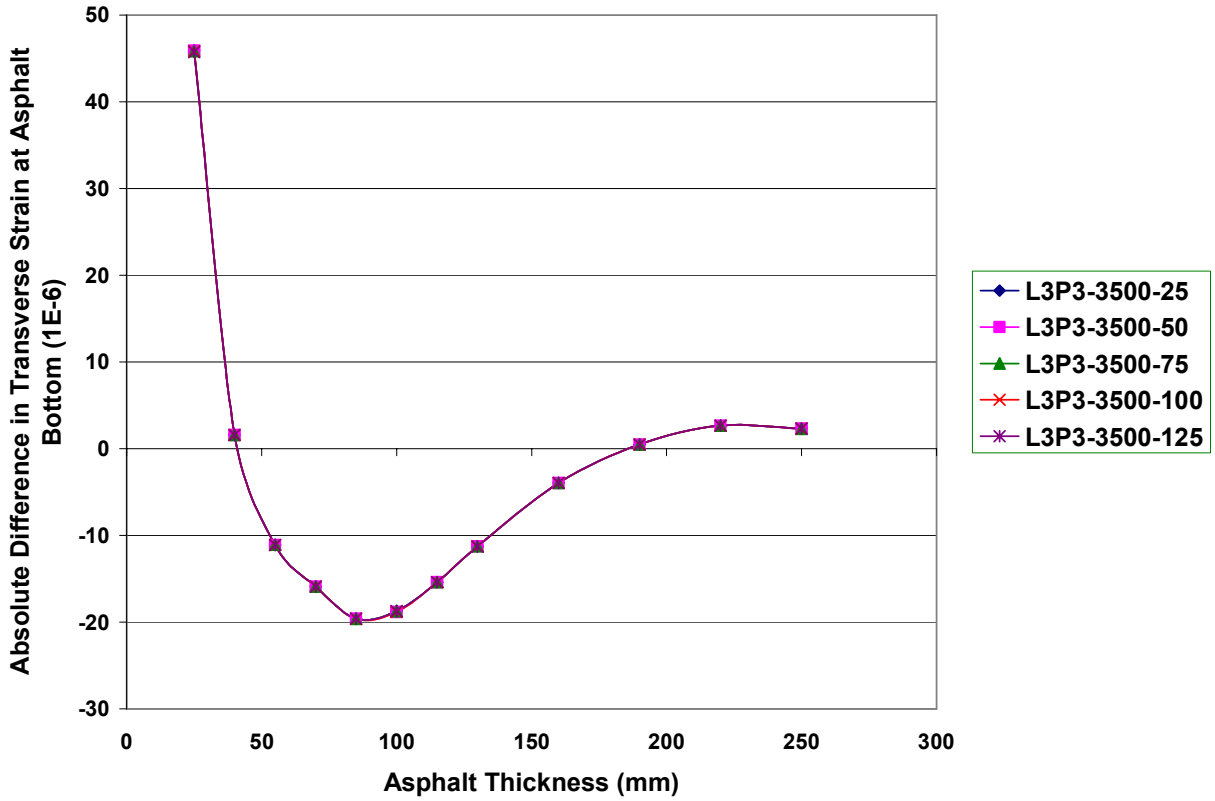

Figure 3.14. Differences in Critical Transverse Tensile Strains at Asphalt Bottom Predicted by 3-D Stress Model and Uniform Stress Model (B)

Figure 3.15 illustrates D_ε in longitudinal strains at pavement surface. When the asphalt layer is not thicker than 55 mm, the uniform stress model underestimates D_ε in longitudinal strains. When asphalt layer is between 85 mm and 130 mm, the uniform stress model overestimates D_ε in longitudinal strains, and the absolute value of D_ε is larger than 10 micros. When the asphalt thickness is between 55 mm and 70 or is larger than 130 mm, the uniform stress model produces similar longitudinal strains to the 3-D stress model.

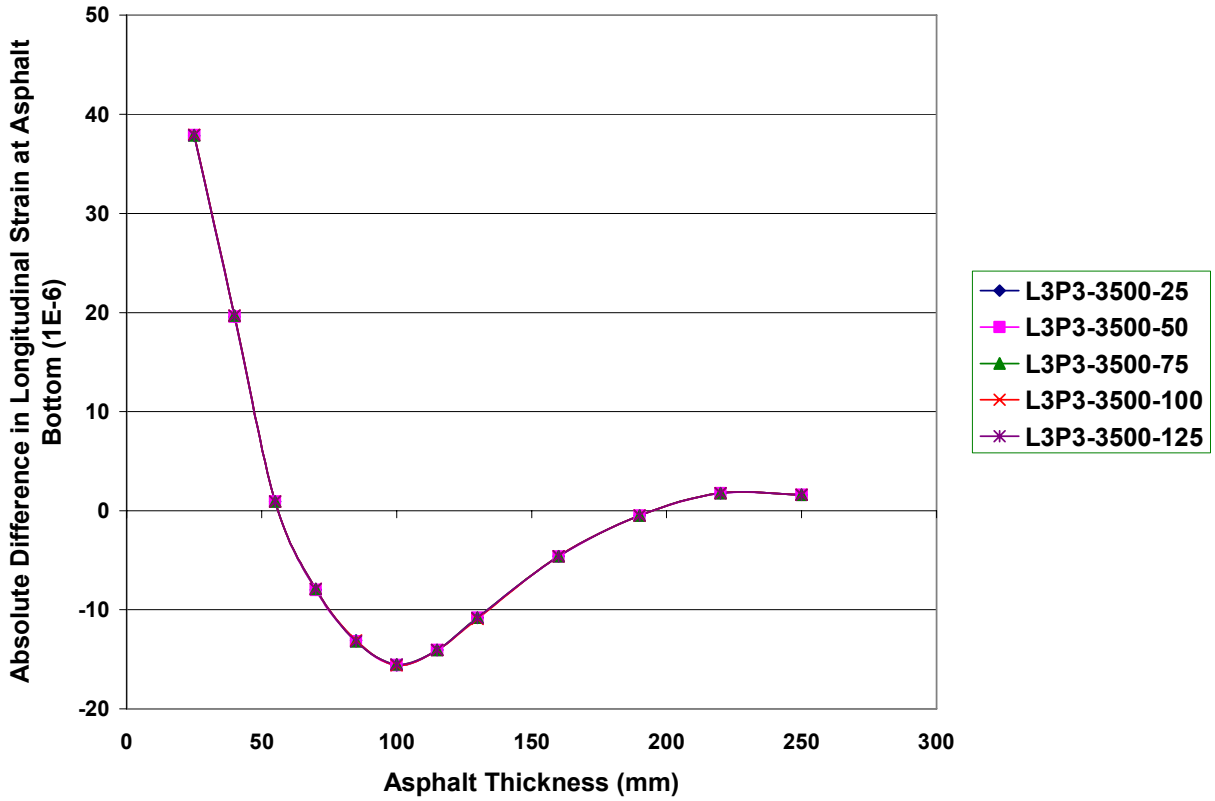

Figure 3.15. Differences in Critical Longitudinal Tensile Strains at Asphalt Bottom Predicted by 3-D Stress Model and Uniform Stress Model (B)

Figure 3.16 indicates that asphalt thickness does not have significant effect on D_ε in vertical strains at the top of subgrade. The magnitude of D_ε varies from -2.5 micros to 0.5 micro. The uniform stress model and the 3-D stress model calculate similar vertical strains at subgrade top regardless of the asphalt thickness and the subgrade modulus.

In summary, Figures 3.12 to 3.16 present the effects of subgrade modulus and asphalt thickness on D_ε in horizontal strains in the asphalt layer and vertical strains at the top of the subgrade. Subgrade modulus does not show significant effect on D_ε in all studied strains. Asphalt thickness shows important effect on D_ε in asphalt strains but not on D_ε in vertical strains at subgrade top.

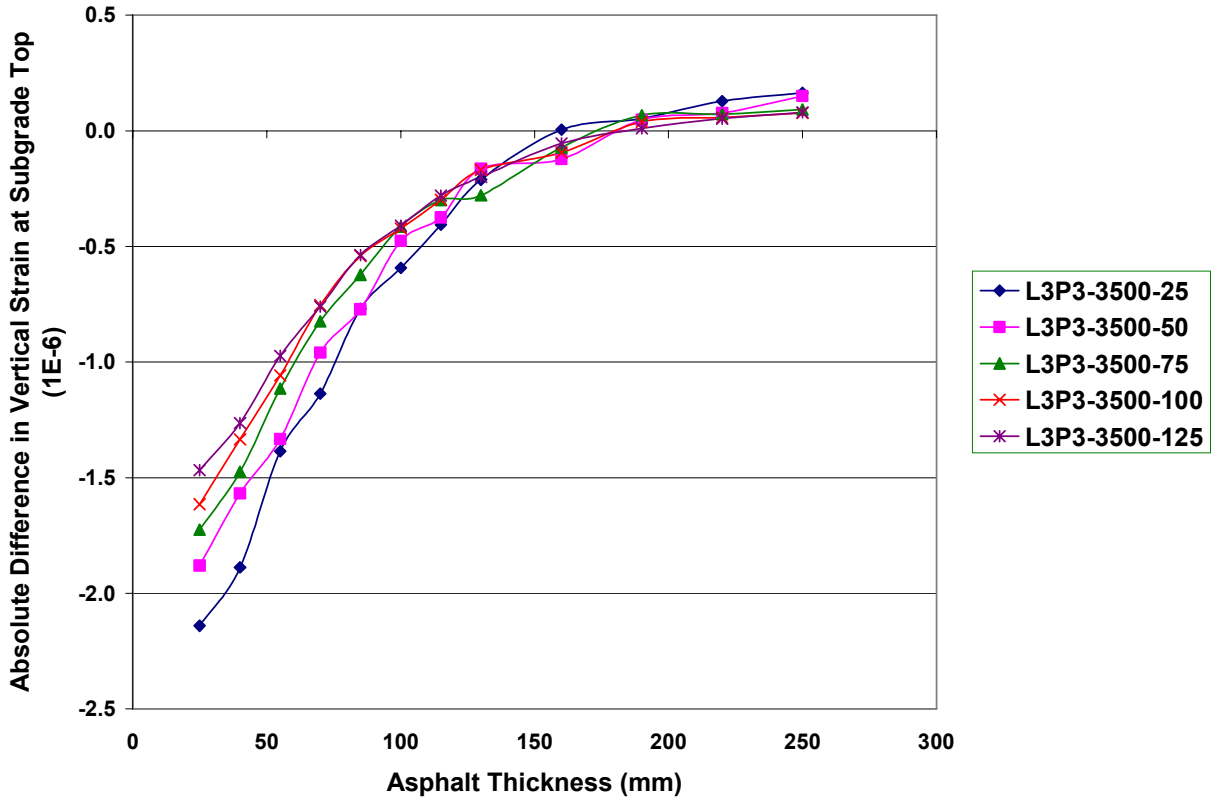

Figure 3.16. Differences in Critical Vertical Strains at Subgrade Top Predicted by 3-D Stress Model and Uniform Stress Model (B)

3.3.3 Effects of Tire Load, Tire Pressure and Asphalt Thickness

The effects of tire load, tire inflation pressure and asphalt thickness on D_ε in studied strains are shown in Figures 3.17 to 3.21. In these five figures, the asphalt modulus has constant value of 3,500 MPa, and the subgrade modulus is also constant and has a magnitude of 75 MPa. The five figures present critical strains at 3 tire load levels and 3 tire inflation pressure levels. In each figure, the same line type represents the same tire load level, and the same marker symbolizes the same tire pressure level. The caption of each figure has a capital letter "C" at the end, which indicates that the figure is in Group C.

Figure 3.17 shows D_ε in transverse strains at pavement surface. When the asphalt layer is not thicker than 55 mm, D_ε has a negative value in most cases, which indicates that the uniform stress model overestimates D_ε in transverse strains at pavement surface under most

combinations of tire load and tire pressure. For the pavement with a thin asphalt layer (< 55 mm), the lower tire pressure is usually associated with a smaller absolute value of D_ε since the same markers group together in Figure 3.17. The effect of tire load on D_ε is not consistent when the asphalt is thinner than 55 mm: at tire pressure level 1, a higher load is associated with a larger absolute value of D_ε; at tire pressure levels 3 and 5, a lower load is associated with a larger absolute value of D_ε. When the asphalt is thicker than 55 mm, the magnitude of D_ε is within ±10 micros in most cases, which implies that critical strains calculated by the uniform stress model are close to those computed by the 3-D stress model.

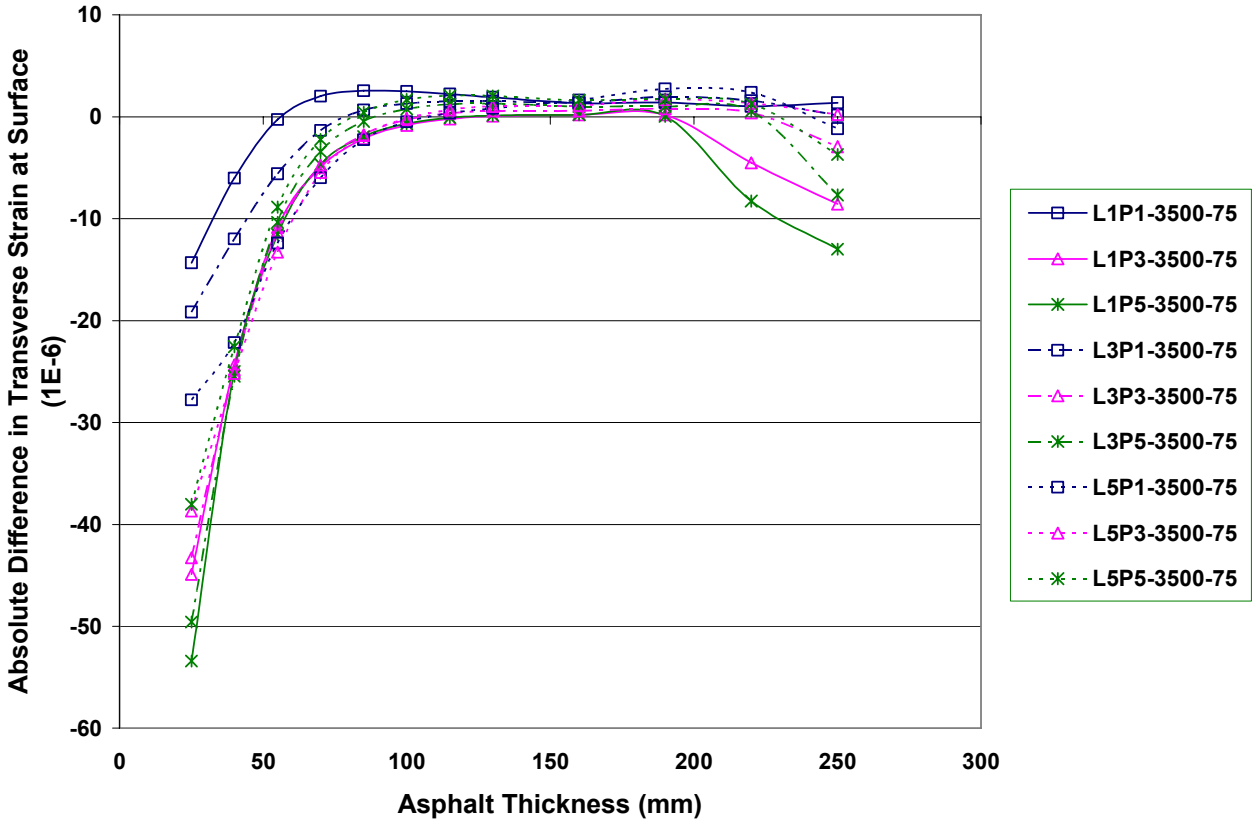

Figure 3.17. Differences in Critical Transverse Tensile Strains at Pavement Surface Predicted by 3-D Stress Model and Uniform Stress Model (C)

Figure 3.18 presents D_ε in longitudinal strains at pavement surface. When the asphalt layer is thinner than 70 mm, D_ε is smaller than -10 micros in most cases; when the asphalt layer is

between 70 mm and 190 mm, D_ε varies in a range of ±10 micros in most cases; when the asphalt layer is thicker than 190 mm, D_ε is larger than 10 micros with only one exception (L3P1). For a pavement with a thin asphalt layer (25 mm), a higher tire pressure is associated with a smaller value of D_ε. The effect of tire load is not very clear in Figure 3.18.

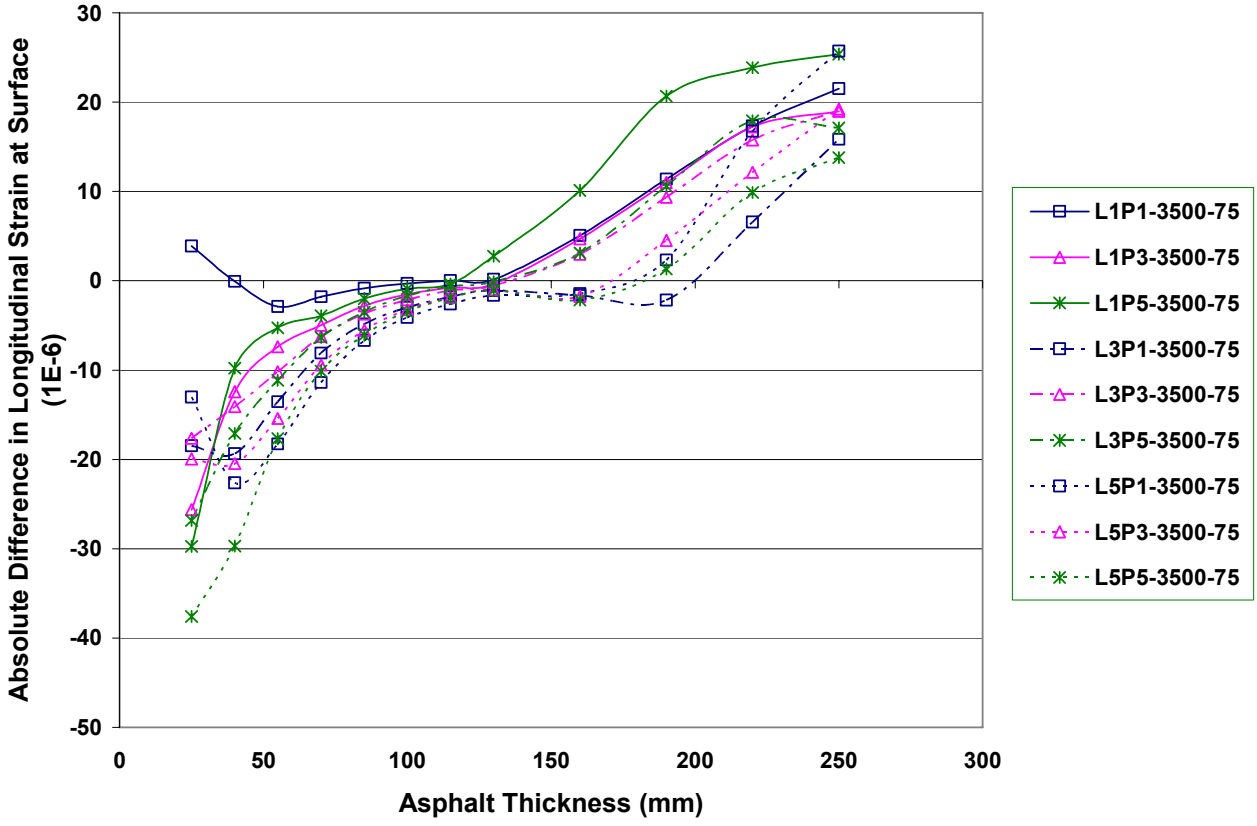

Figure 3.18. Differences in Critical Longitudinal Tensile Strains at Pavement Surface Predicted by 3-D Stress Model and Uniform Stress Model (C)

Figure 3.19 illustrates D_ε in transverse strains at the bottom of asphalt layer. As compared to Figure 3.20, D_ε in most cases are larger than that in the longitudinal strains because the uniform stress model produces symmetric horizontal strains, and due to the 3-D stress model, transverse strains in most cases are more critical than longitudinal strains. At the same tire pressure level, a higher tire load is associated with a larger D_ε; at the same tire load level, a lower tire pressure is accompanied with a larger D_ε. For thin asphalt layers (< 40 mm), most transverse strains are

underestimated by the uniform stress model, and D_ε in transverse strains can be as high as close to 200 micros. If the asphalt thickness is larger than 160 mm, two models produce similar critical transverse strains. When the asphalt thickness is between 40 mm and 160 mm, the uniform stress model underestimates the transverse strains under high tire load and low tire pressure. Therefore, the uniform stress model may not be appropriate for predicting the transverse strain in a combination of thin asphalt layer, high tire load and low tire pressure.

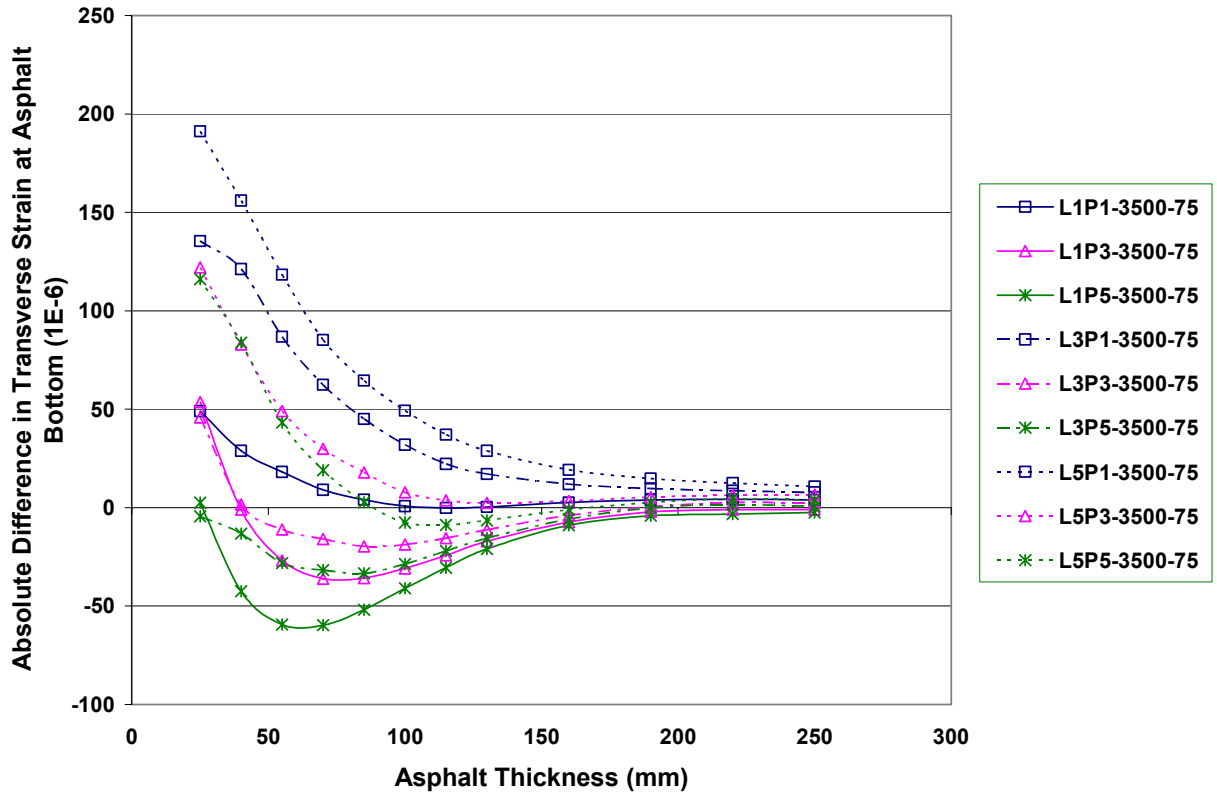

Figure 3.19. Differences in Critical Transverse Tensile Strains at Asphalt Bottom Predicted by 3-D Stress Model and Uniform Stress Model (C)

Figure 3.20 shows D_ε in longitudinal strains at asphalt bottom. At the same tire load level, the lower tire pressure is associated with a larger D_ε. At tire pressure level 1, a lower tire load is associated with a larger D_ε; at tire pressure level 5, a lower tire load is associated with a lower D_ε. When the asphalt layer less than 40 mm thick, the uniform stress model underestimates the critical longitudinal strains at the asphalt bottom in most cases since the magnitude of D_ε is

positive in most cases. This observation indicates that the uniform stress model is neither safe nor accurate for the design of pavements with thin asphalt surfaces. When the asphalt layer is thicker than 130 mm, the uniform stress model and the 3-D stress model produce similar critical tensile strains in the longitudinal direction. If the asphalt layer is between 40 mm and 130 mm, the uniform stress model overestimates the longitudinal tensile strains in most cases except where tire pressure is low. As a result, the uniform stress model may not accurately predict the longitudinal tensile strains at asphalt bottom in a combination of thin asphalt layer and low tire pressure.

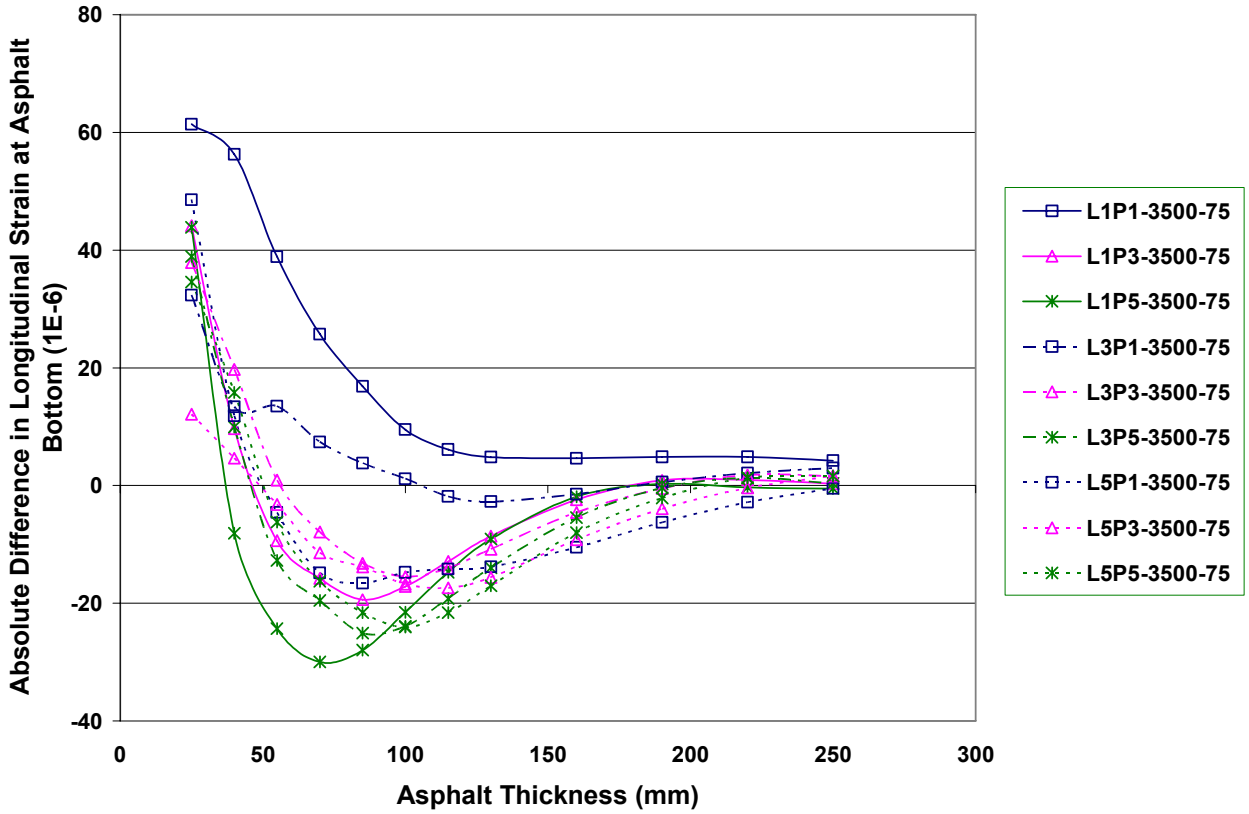

Figure 3.20. Differences in Critical Longitudinal Tensile Strains at Asphalt Bottom Predicted by 3-D Stress Model and Uniform Stress Model (C)

Figure 3.21 presents D_ε in vertical strains at the top of subgrade. A lower tire pressure is associated with a larger D_ε, and a lower tire load is accompanied with a smaller D_ε. Since the

magnitude of D_ε in vertical strains at subgrade top is within ± 4 micros, the uniform stress model and the 3-D stress model produce similar critical vertical strains at the top of subgrade.

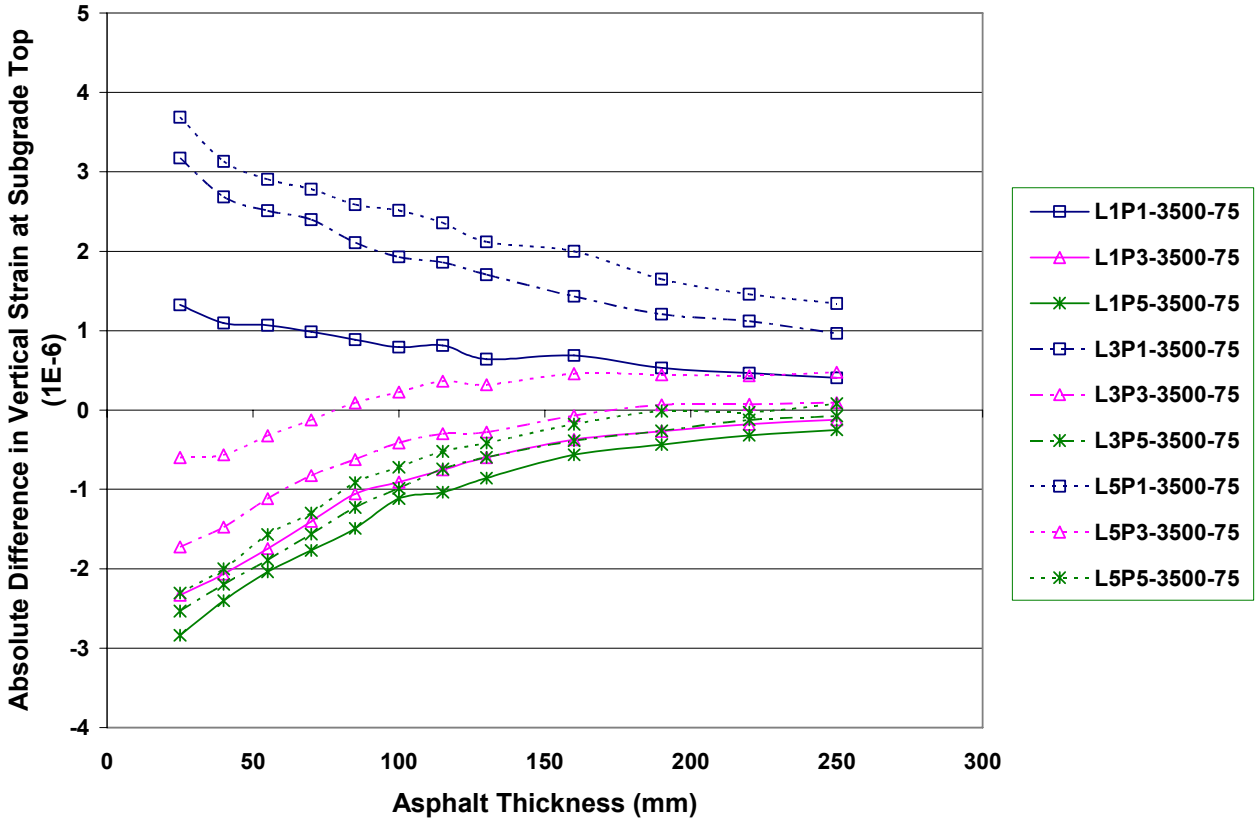

Figure 3.21. Differences in Critical Vertical Strains at Subgrade Top Predicted by 3-D Stress Model and Uniform Stress Model (C)

Chapter 4 Pavement Performance Prediction

4.1 Distress Models

Distress models are also called transfer functions, which are used to predict pavement distresses by pavement structural responses (Huang, 2004). Transfer functions are well developed for the fatigue cracking of Hot Mixed Asphalt (HMA) and subgrade rutting. This chapter will focus on the fatigue crack models for the asphalt layer. The pavement fatigue life in terms of the allowable number of load repetitions will be predicted by different distress models using pavement strains calculated by both 3-D stress model and uniform stress model. The subgrade rutting will not be discussed in this chapter because the uniform stress model and 3-D stress model produce similar vertical strains at the top of subgrade. As a result, the two models will lead to similar subgrade rutting.

The most well-known fatigue cracking models are the Asphalt Institute and Shell Design methods. These two methods relate the allowable number of load repetitions leading to fatigue cracking to the tensile strain at the bottom of the asphalt layer and to the asphalt modulus. Equation 4.1 is the basic form of these two models:

$$N_f = f_1(\varepsilon_t)^{-f_2}(E_1)^{-f_3} \tag{4.1}$$

in which:

N_f = allowable number of load repetitions to cause fatigue cracking;

ε_t = tensile strain at the bottom of the asphalt layer;

E_1 = the modulus of the asphalt layer; and

f_1, f_2 and f_3 = parameters.

The Asphalt Institute equation is (Huang, 2004):

$$N_f = 0.0796(\varepsilon_t)^{-3.291}(E_1)^{-0.854} \tag{4.2}$$

The Shell equation is (Huang, 2004):

$$N_f = 0.0685(\varepsilon_t)^{-5.671}(E_1)^{-2.363} \tag{4.3}$$

The tensile strains at asphalt bottom predicted in Chapter 3 and the corresponding asphalt modulus are plugged into Equations 4.2 and 4.3 to calculate the allowable number of load repetitions. The tensile strains used in the two equations are predicted by either the 3-D stress model or the uniform stress model. Since there is a difference in tensile strains at the asphalt bottom calculated by the 3-D stress model and the uniform stress model, the predicted fatigue lives are different if using tensile strains from different stress models. All the differences in fatigue lives are calculated by Equation 4.4. According to this equation, a positive value of D_N indicates that the fatigue life calculated based on the tensile strains from the 3-D stress model is longer than that based on the tensile strains from the uniform stress model, and vise versa.

$$D_N = N_{fn} - N_{fu} \tag{4.4}$$

where:

D_N = difference in fatigue lives caused by different tensile strains at the bottom of the asphalt layer;

N_{fn} = allowable number of load repetitions predicted using tensile strains from the 3-D non-uniform stress model; and

N_{fu} = allowable number of load repetitions predicted using tensile strains from the uniform stress model.

According to the calculation results of the pavement fatigue life, the Asphalt Institute method produces reasonable allowable number of load repetitions. However, the allowable number of load repetitions predicted by the Shell method is unreasonably large in each studied case. Therefore, the following section will focus on the pavement life predicted by the Asphalt Institute method. The pavement life predicted by the Shell method is reported in Appendix 2.

4.2 Pavement Life Predicted by Asphalt Institute Method

A number of figures are plotted to illustrate the pavement fatigue life predicted by the Asphalt Institute method in selected cases with differing tire load and tire pressure. Figures are also plotted to show the difference in fatigue lives according to different tensile strains calculated by the 3-D stress model and the uniform stress model. In total, nine figures are presented in this

section. Figures 4.1 to 4.3 exhibit the effects of tire load and asphalt thickness on the fatigue life; Figures 4.4 to 4.6 illustrate the effects of tire pressure and asphalt thickness on the fatigue life; and Figures 4.7 to 4.9 display the combined effect of tire load, tire pressure and asphalt thickness on fatigue life. In Figures 4.1, 4.2, 4.4, 4.5, 4.7 and 4.8, the allowable number of load repetitions (vertical axis) is displayed in a logarithmic scale in order to make the figures more clear. In Figures 4.3, 4.6 and 4.9, the number of load repetitions (vertical axis) has a display unit in millions.

4.2.1 Effect of Tire Load and Asphalt Thickness

Figure 4.1 shows the pavement fatigue life predicted by the Asphalt Institute method using tensile strains calculated by the 3-D stress model. In this figure, the tire load has five different levels, while the tire pressure, asphalt modulus and subgrade modulus have constant values. Therefore, the effects of the tire load and the asphalt thickness can be shown in this figure. Except for the case of Load Level 1 (L1P3-3500-75), the allowable numbers of load repetitions in the other four cases increase initially and then decrease as the asphalt thickness increases. If the asphalt thickness is greater than some critical value, the allowable number of load repetitions monotonically increases as the asphalt thickness increases. This phenomenon can be explained by the confinement effect of tire on pavement surface: when the asphalt layer is very thin compared to the tire-pavement contact area, the tire has a significant confinement effect on the pavement. As a result, tensile strains do not fully develop. The asphalt thickness also impacts the effect of tire load on the number of load repetitions. When the asphalt layer is thicker than 115 mm, the lower load level is associated with a larger number of load repetitions. When the asphalt thickness is less than 115 mm, the effect of tire load is not very clear in Figure 4.1.

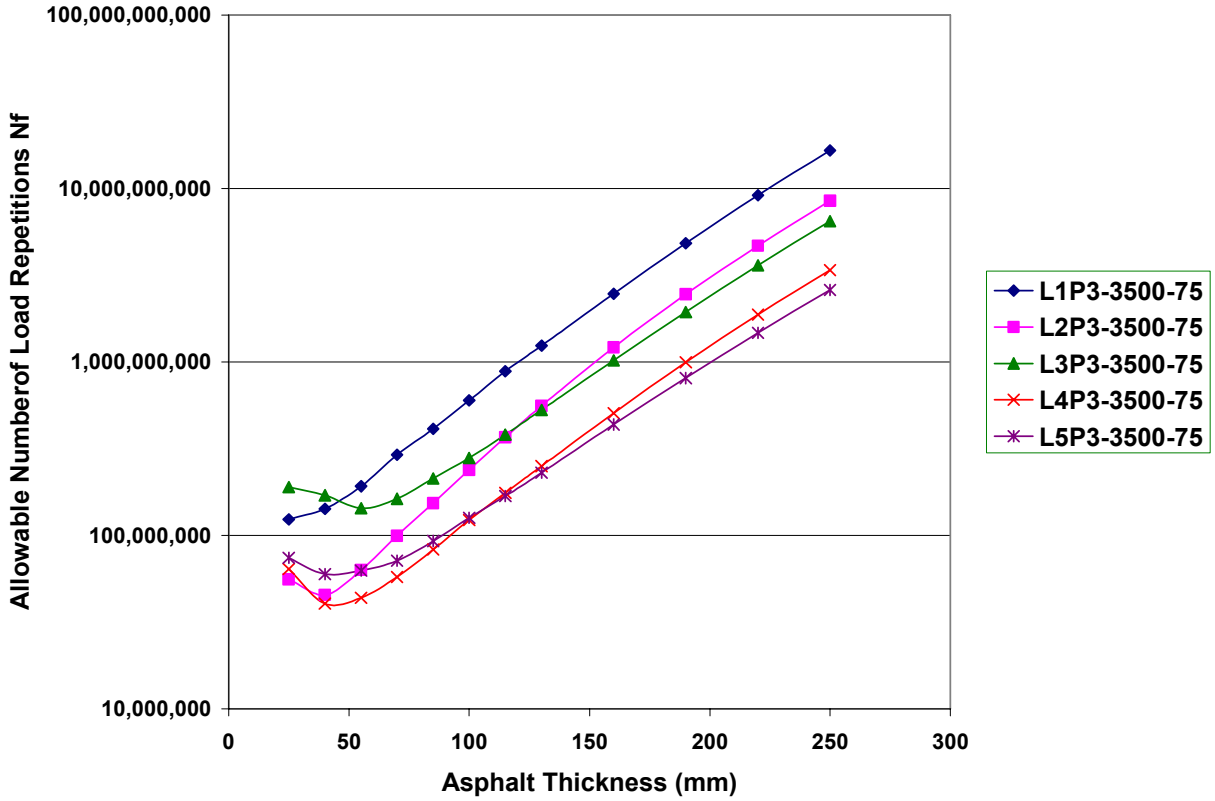

Figure 4.1. Effects of Tire Load on Pavement Fatigue Life Predicted by Asphalt Institute Method Based on Tensile Strains Calculated by 3-D Stress Model

Figure 4.2 displays the fatigue life predicted by the Asphalt Institute method based on tensile strains computed by the uniform stress model. As in Figure 4.1, Figure 4.2 has five levels of tire load and constant levels of tire pressure, asphalt modulus and subgrade modulus. Similar to Figure 4.1, the allowable numbers of load repetitions in all cases increase initially and then decrease as the asphalt thickness increases. When the asphalt layer is thicker than a critical value (around 60 mm as shown in Figure 4.2), the numbers of load repetitions monotonically increase as the asphalt thickness increases. Meanwhile, when the asphalt layer is thicker than the critical value (around 60 mm), a lower tire load is associated with a higher number of load repetitions, which indicates that the pavement has a longer fatigue life if the tire load is lower. On the contrary, if the asphalt thickness is less than this critical value, a higher tire load is accompanied by a higher number of load repetitions. This observation implies that a pavement with a thin asphalt layer has a longer fatigue life when heavier tire loads are applied to the pavement surface.

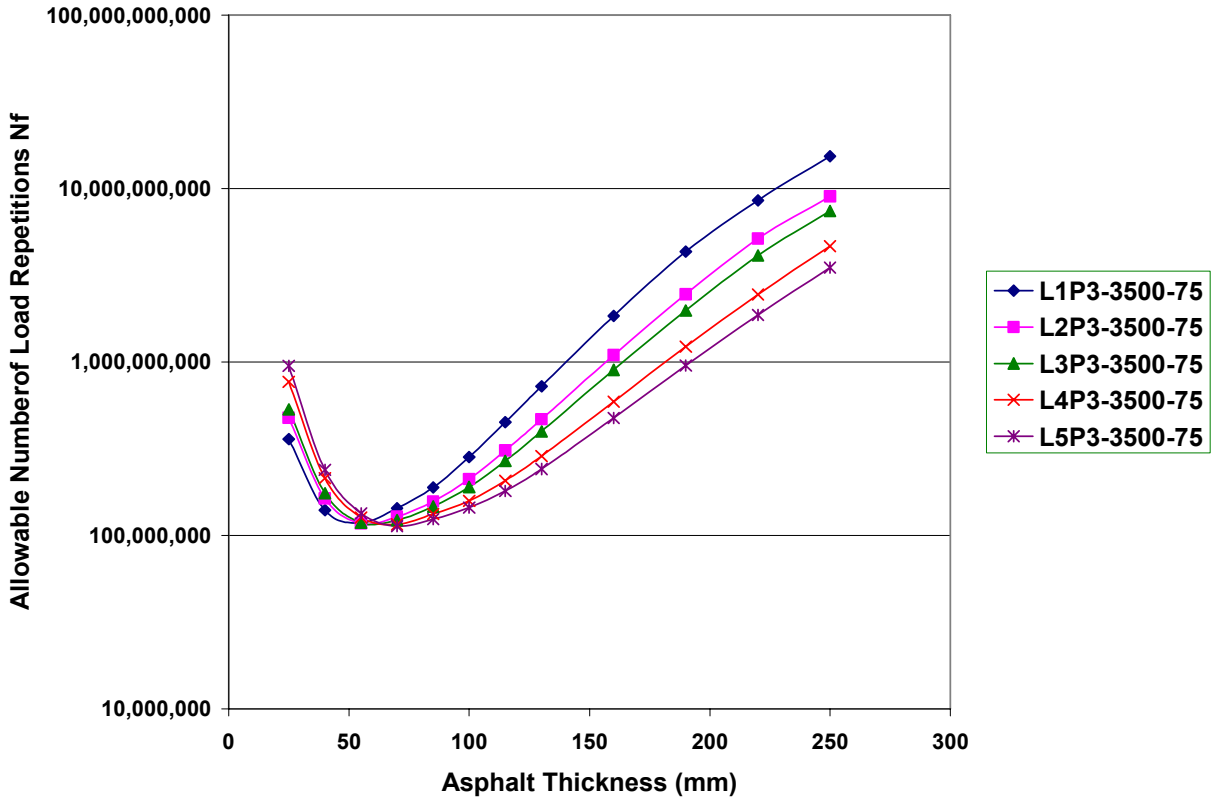

Figure 4.2. Effects of Tire Load on Pavement Fatigue Life Predicted by Asphalt Institute Method Based on Tensile Strains Calculated by Uniform Stress Model

Figure 4.3 illustrates the difference in the allowable numbers of load repetitions (D_N) according to the difference in tensile strains calculated by the 3-D stress model and the uniform stress model. D_N is computed using Equation 4.4. In this figure, tire load has five levels, and tire pressure, asphalt modulus and subgrade modulus have constant levels. When the tire load is at the lowest level, D_N has a positive value when the asphalt layer is thicker than 40 mm, and D_N can be higher than 1,200 million with the increase of the asphalt thickness. When the asphalt layer is thinner than 40 mm, D_N has a negative value in all five cases. When the asphalt thickness is between 40 mm and 190 mm, D_N varies in a range of ±250 million for the cases with Load Levels 2, 3, 4 and 5. If the asphalt is thicker than 220 mm, D_N has a value of less than -500 million in most cases. These facts indicate that, when the asphalt layer is very thin (< 40 mm) or very thick (>220 mm), the predicted pavement fatigue life based on the tensile strains

from the 3-D stress model is shorter than that based on the tensile strains from the uniform stress model.

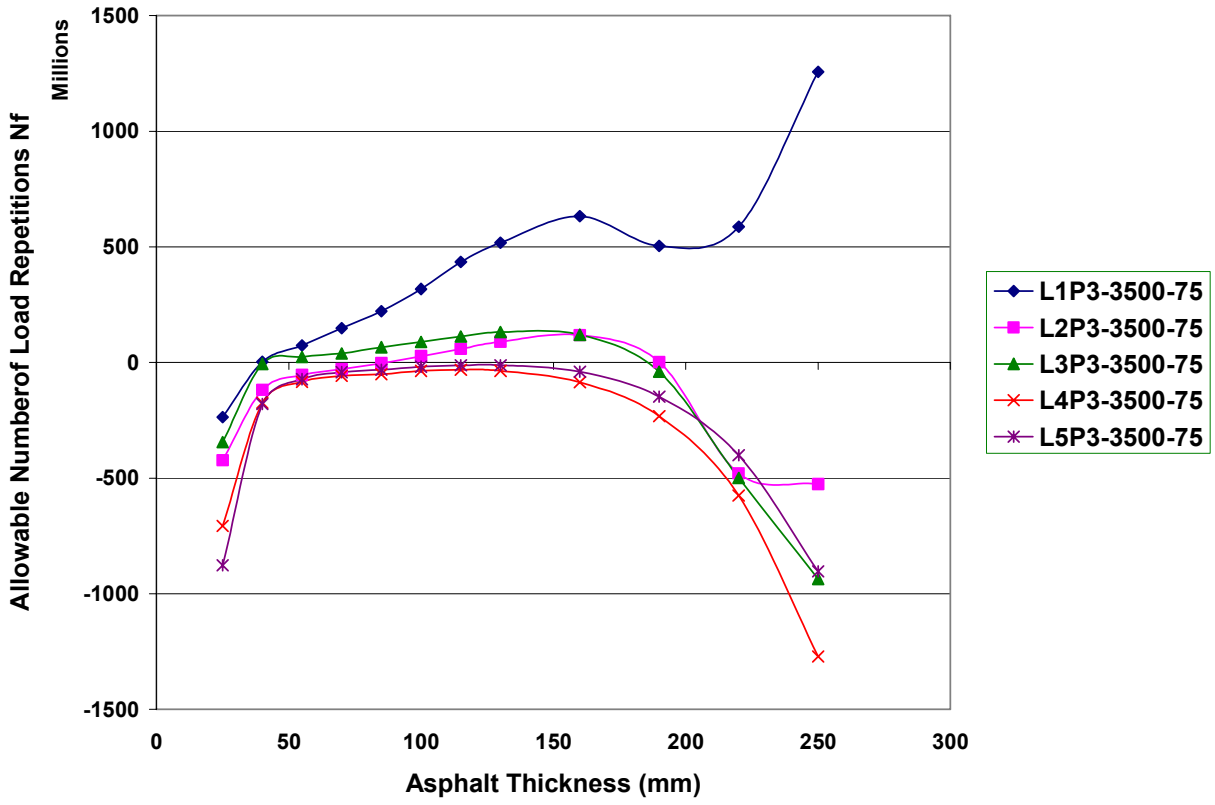

Figure 4.3. Differences in Number of Load Repetitions According to Differences in Tensile Strains Predicted by 3-D Stress Model and Uniform Stress Model (Varying Tire Load)

4.2.2 Effect of Tire Pressure and Asphalt Thickness

Figure 4.4 presents the pavement fatigue life using tensile strains computed by the 3-D stress model with different tire pressure levels. In this figure, the tire pressure has five different levels, and the tire load, asphalt modulus and subgrade modulus have constant values. The effect of tire pressure on the number of load repetitions is not very clear in Figure 4.4, in which the highest tire pressure is associated with the smallest number of load repetitions when the asphalt thickness is larger than a critical value, while Tire Pressure Level 3 is accompanied by the largest number of load repetitions in all cases. On the contrary, the effect of tire pressure is very clear in Figure 4.5, in which the pavement fatigue lives are calculated based on the tensile strains from the

uniform stress model. In most cases, a higher tire pressure is associated with a smaller number of load repetitions.

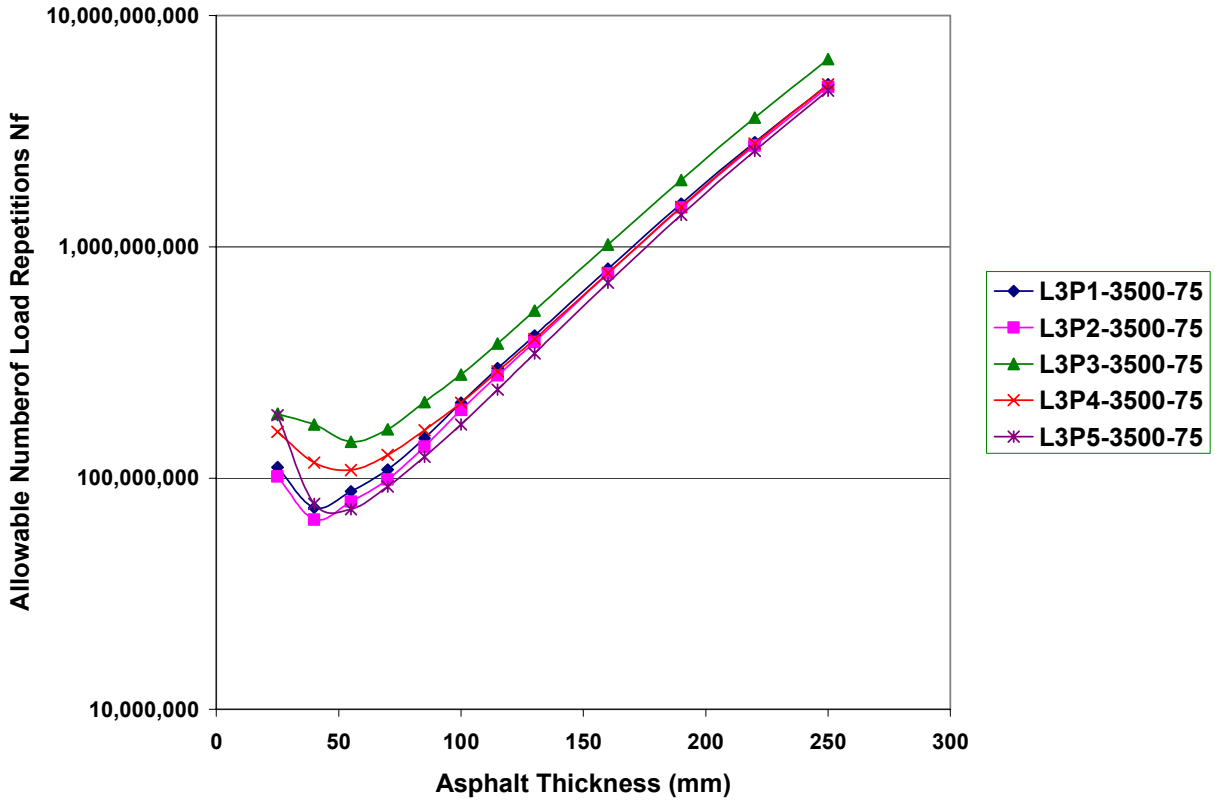

Figure 4.4. Effects of Tire Pressure on Pavement Fatigue Life Predicted by Asphalt Institute Method Based on Tensile Strains Calculated by 3-D Stress Model

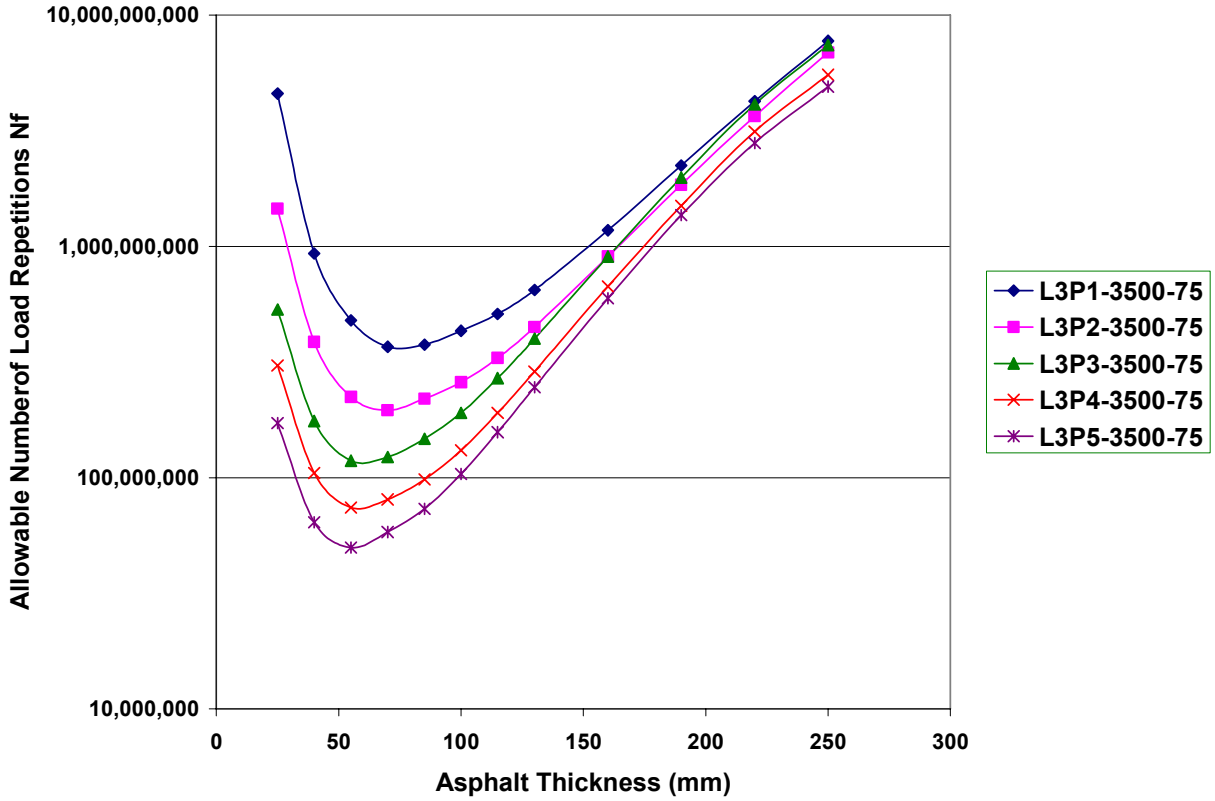

Figure 4.5. Effects of Tire Pressure on Pavement Fatigue Life Predicted by Asphalt Institute Method Based on Tensile Strains Calculated by Uniform Stress Model

Figure 4.6 illustrates the difference in numbers of load repetitions according to the difference in tensile strains predicted by the 3-D stress model and the uniform stress model. Figure 4.6, which has different tire pressure levels, is different from Figure 4.3, which has different tire load levels. As shown in Figure 4.6, a lower tire pressure is associated with a smaller value of D_N. This fact indicates that the 3-D stress model leads to a shorter pavement fatigue life than the uniform stress model. When the asphalt thickness is between 55 mm and 160 mm, the magnitude of D_N is within ±400 million. If the asphalt layer is thinner than 55 mm or thicker than 160 mm, D_N has a lower value in most cases.

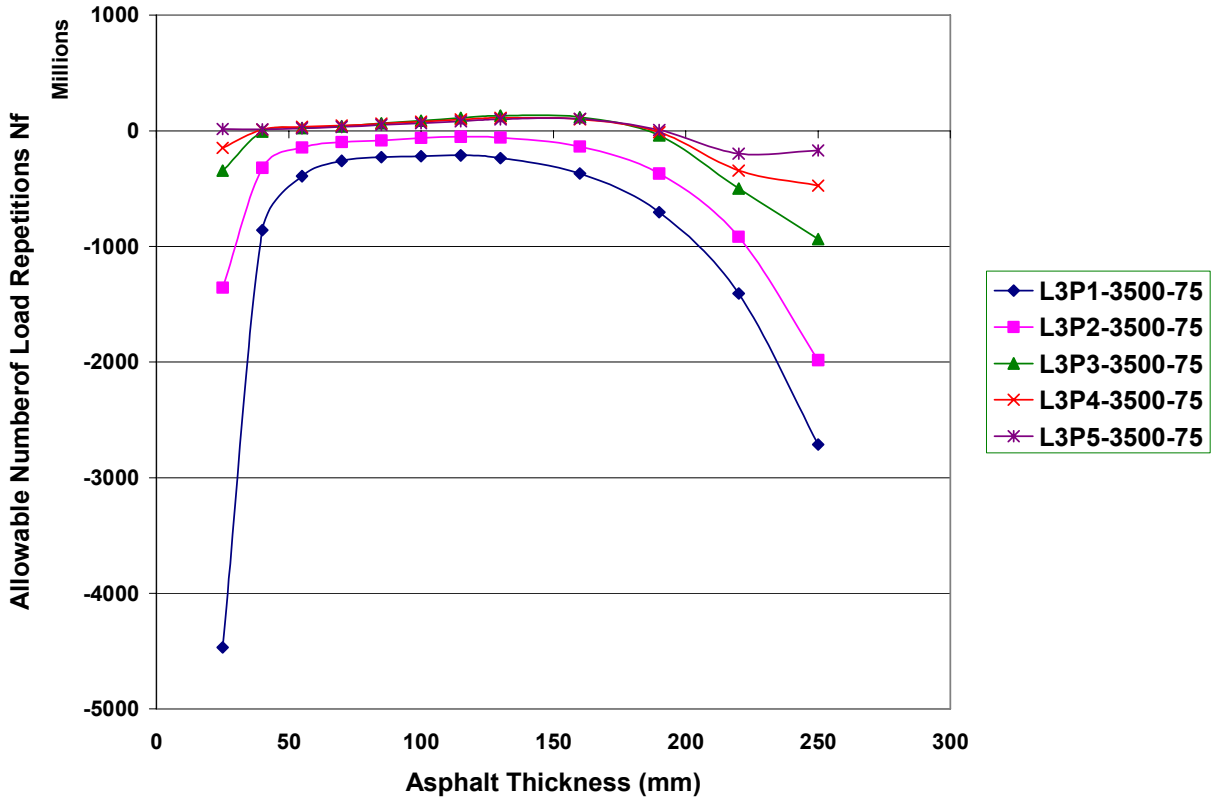

Figure 4.6. Differences in Number of Load Repetitions According to Differences in Tensile Strains Predicted by 3-D Stress Model and Uniform Stress Model (Varying Tire Pressure)

4.2.3 Effect of Tire Load, Tire Pressure and Asphalt Thickness

In order to compare the effects of tire load and tire pressure, a number of cases are selected with different tire load levels and tire pressure levels. In Figures 4.7, 4.8 and 4.9, the same line type represents the same tire load level, and the same marker symbolizes the same tire pressure level.

Figure 4.7 shows predicted fatigue life based on the tensile strains calculated by the 3-D stress model. As can be seen from this figure, the curves with the same line type group together, which indicates that the effect of the tire load is larger than the effect of the tire pressure on the pavement fatigue life. In most cases, a lower tire load level is associated with a larger number of load repetitions. At Tire Load Levels 1 and 3, Tire Pressure Level 3 is associated with the largest number of load repetitions in most cases, and Tire Pressure Level 5 is accompanied by the

smallest number of load repetitions in most cases. At Tire Load Level 5, a larger tire pressure is associated with a smaller number of load repetitions in most cases.

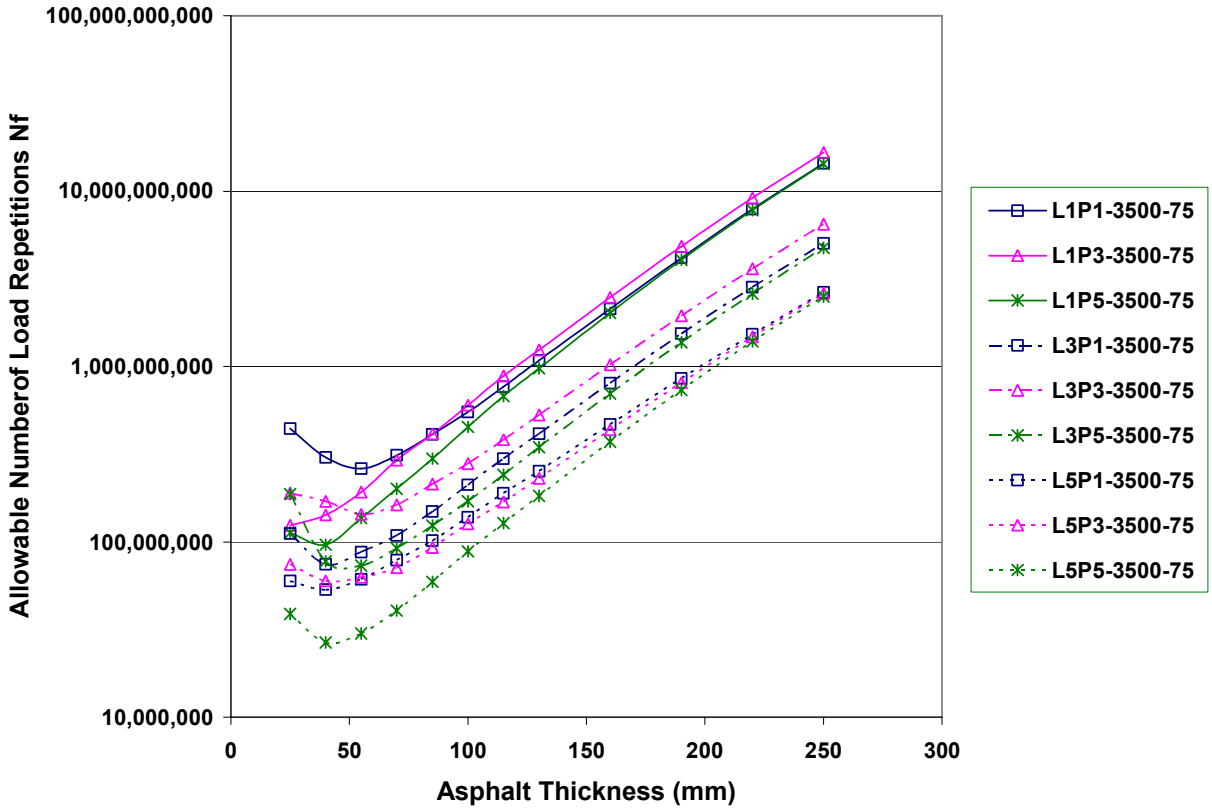

Figure 4.7. Effects of Tire Load and Tire Pressure on Pavement Fatigue Life Predicted by Asphalt Institute Method Based on Tensile Strains Calculated by 3-D Stress Model

Figure 4.8 shows the predicted numbers of load repetitions according to the tensile strains computed by the uniform stress model. As shown in Figure 4.8, when the asphalt thickness is smaller than some value, the same markers group together. This fact indicates that the effect of tire pressure on pavement fatigue life is larger than the effect of tire load when the pavement has a thin asphalt layer. Meanwhile, when the asphalt layer is thinner than a critical value, a larger tire load is associated with a larger number of load repetitions; when the asphalt thickness is larger than this critical value, a larger tire load is accompanied by a smaller number of load repetitions. This critical value varies with the tire pressure. For example, at Tire Pressure Level 1, this critical asphalt thickness is 70 mm; at Tire Pressure Level 3, the critical value is a little larger than 55 mm; and at Tire Pressure Level 5, the critical value is a little less than 55 mm. As a result, a lower tire pressure level is associated with a larger critical asphalt thickness. As the

asphalt thickness increases, the effect of tire load on pavement fatigue life gradually increases, and the effect of tire pressure decreases. As shown in Figure 4.8, when the asphalt thickness is larger than some value, the same line types group together. This observation indicates that the effect of tire load on pavement fatigue life is greater than the effect of tire pressure when the pavement has a thick asphalt layer. The results shown in Figure 4.8 follow engineering principles.

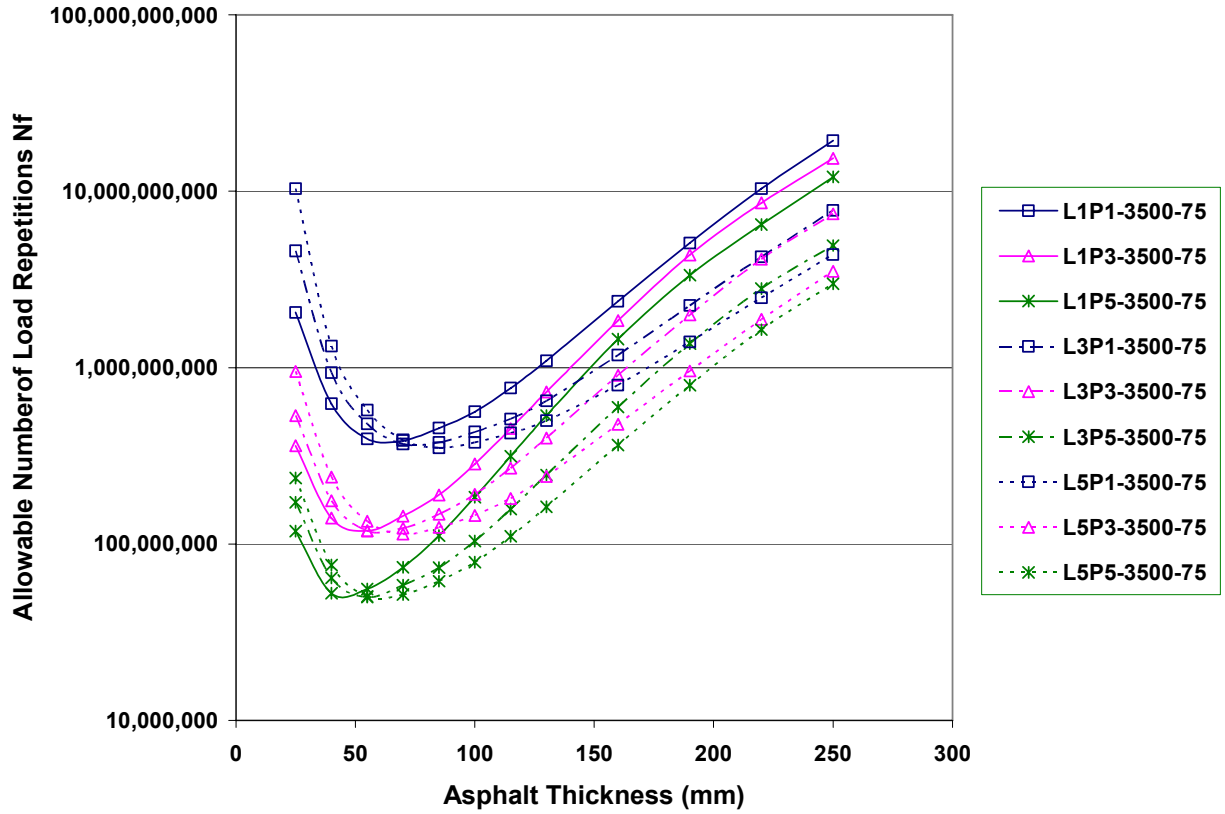

Figure 4.8. Effects of Tire Load and Tire Pressure on Pavement Fatigue Life Predicted by Asphalt Institute Method Based on Tensile Strains Calculated by Uniform Stress Model

Figure 4.9 displays the difference in numbers of load repetitions according to the difference in tensile strains calculated by the 3-D stress model and the uniform stress model. Nine cases with three levels of tire load and three levels of tire pressure are selected to show the effects of tire load and tire pressure on D_N. As shown in Figure 4.9, Tire Pressure Level 1 is associated with the smallest D_N at all tire load levels. When the asphalt layer is thinner than 70 mm, tire pressure has a greater effect on D_N than tire load since the same markers group together in

Figure 4.9; at each tire pressure level, a smaller tire load is accompanied by a larger D_N. When the asphalt thickness is between 70 mm and 160 mm, the magnitude of D_N in each case is closer to zero. When the asphalt is thicker than 160 mm, a higher tire pressure is associated with a larger D_N at each tire load level; meanwhile, at Tire Pressure Level 1, a smaller tire load is accompanied by a smaller D_N, and at Tire Pressure Level 5, a smaller tire load is associated with a larger D_N. All cases with Tire Pressure Level 1 have negative values of D_N, which indicates that the 3-D stress model leads to a smaller number of load repetitions than the uniform stress model when the tire pressure is at a relatively low level.

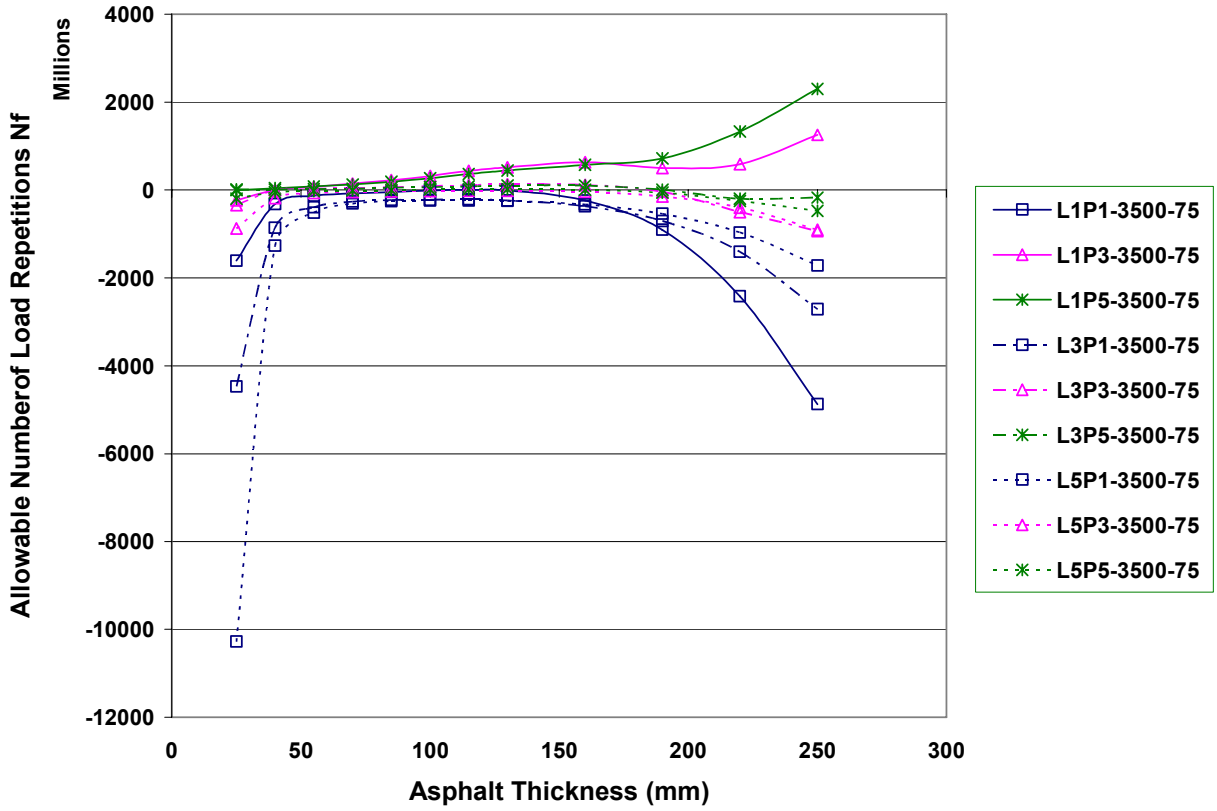

Figure 4.9. Differences in Number of Load Repetitions According to Differences in Tensile Strains Predicted by 3-D Stress Model and Uniform Stress Model (Varying Tire Load and Tire Pressure)

Chapter 5 Conclusions

This research incorporates the measured 3-D non-uniform tire-pavement contact stresses as well as the traditional uniform contact stresses to study pavement responses and performance. Multi-layer linear elastic program, CIRCLY, is used to simulate measured 3-D stress and uniform stress. The experimental design includes five variables: i) 12 asphalt layer thicknesses; ii) five levels of tire load; iii) five levels of tire pressure; iv) five levels of asphalt modulus; and v) five levels of subgrade modulus.

The analysis evaluates the individual and combined effects of the 3-D stress components (vertical stress, longitudinal stress and transverse stress) on the distributions of pavement strains within and close to the contact area at pavement surface, the bottom of the asphalt layer, and the top of subgrade. The studied pavement strains include: i) longitudinal and transverse strains at pavement surface; ii) longitudinal and transverse strains at the bottom of the asphalt layer; and iii) vertical strains at the top of subgrade. Every strain distribution is graphically presented in three dimensions using MATLAB software. The strain distributions as well as the critical values of all strain distributions calculated by the 3-D stress model are compared to those estimated by the uniform stress model in order to evaluate the possible errors caused by the assumptions in the traditional uniform stress model.

Two pavement distress models, the Asphalt Institute method and the Shell method, are used to predict pavement fatigue life based on the tensile strains calculated by both 3-D stress model and the uniform stress model. The pavement fatigue life results predicted by the Asphalt Institute method are analyzed in detail. The fatigue life results predicted by the Shell method are plotted in Appendix 2. The effects of tire load and tire pressure on pavement fatigue life are reported and compared at different asphalt thickness levels.

The major findings of this study are summarized as follows:

- Among the three stress components of the measured 3-D contact stresses, the vertical stress has the dominant effect on the horizontal strains in both directions at

pavement surface and at the bottom of the asphalt layer, and on the vertical strains at the top of subgrade. Although the effects of longitudinal stress component and transverse stress component are secondary to the effect of the vertical stress component, they are significant and cannot be ignored, especially for thinner pavements which constitute the vast majority of Texas' road network.

- Under the 3-D stresses, both longitudinal and transverse strains at the pavement surface are compressive strains within the contact area and are tensile strains at the edge or adjacent to the contact area. As the asphalt thickness increases, the horizontal tensile strains tend to decrease under the combined effect of 3-D stresses.
- Under the 3-D stresses, when the asphalt layer is relatively thin, two peaks of tensile strain distribution develop at the bottom of the asphalt layer within the contact area, and compressive strains develop at the edge and outside of the contact area. The compressive strain may develop around the center of the contact area for pavement with a very thin asphalt layer. As the asphalt thickness increases, the shape of the transverse strain distribution changes from a "w-shape" to a "u-shape".
- Asphalt modulus, asphalt thickness, tire load and tire pressure have significant effect on the differences in strains at pavement surface and at the bottom of the asphalt between the 3-D stress model and the uniform stress model, but not on the differences in strains at the top of subgrade. Subgrade modulus has a slight effect on the differences in all pavement strains predicted by the 3-D stress model and the uniform stress model.
- Tire pressure shows significant effect on the fatigue life of a pavement with a thin asphalt layer. The effect of tire pressure decreases as the asphalt thickness increases. When the asphalt thickness is small, a higher tire load is associated with a larger number of load repetitions in most cases. When the pavement has a thick asphalt layer, a higher tire load is accompanied by a smaller number of load repetitions, and the effect of tire load is larger than the effect of tire pressure.

References

De Beer, M., and Fisher, C. (1997) *Contact Stresses of Pneumatic Tires Measured with the Vehicle-Road Surface Pressure Transducer Array (VRSPTA) System for the University of California at Berkeley (UCB) and the Nevada Automotive Test Center (NATC)*. Research Report No. CR-97/053, Division of Roads and Transport Technology, CSIR, South Africa.

De Beer, M., Fisher, C., and Jooste, F. J. (1997) Determination of Pneumatic Tyre/Pavement Interface Contact Stresses under Moving Loads and Some Effects on Pavements with Thin Asphalt Surfacing Layers. *Proceedings of the 8th International Conference on Asphalt Pavements*, Volume I. Seattle, Washington, pp. 179-227.

De Beer, M., and Fisher, C. (2002) *Tire Contact Stress Measurements with the Stress-In-Motion (SIM) Mk IV System for the Texas Transportation Institute (TTI)*, Part of TxDOT Project 0-4361, Texas A&M University, College Station, Texas.

De Beer, M. (2006) Reconsideration of Tyre-Pavement Input Parameters for the Structural Design of Flexible Pavements. *Proceedings of the 10th International Conference on Asphalt Pavements*, Quebec City, Canada.

El-basyouny, M. M., and Witczak, M. (2005) Development of the Fatigue Cracking Models for the 2002 Design Guide. *The 84th Transportation Research Board Annual Meeting. CD-ROM.* Transportation Research Board, National Research Council, Washington D.C.

Huang, Y. H. (2004) *Pavement Analysis and Design*. Pearson Education, Inc., Upper Saddle River, New Jersey.

Machemehl, R. B., Wang, F., and Prozzi, J. A. (2005) Analytical Study of Effects of Truck Tire Pressure on Pavements Using Measured Tire-Pavement Contact Stress Data. *Transportation Research Record: Journal of the Transportation Research Board,* No. 1919, Transportation Research Board of the National Academies, Washington, D.C., pp. 111-120.

Prozzi, J. A., and Luo, R. (2005) Quantification of the Joint Effect of Wheel Load and Tire Inflation Pressure on Pavement Response. *Transportation Research Record: Journal of Transportation Research Board,* No. 1919, Transportation Research Board of the National Academies, Washington, D.C., pp. 134-141.

Luo, R., and Prozzi, J. A. (2007) Strain Distribution in the Asphalt Layer under Measured 3-D Tire-Pavement Contact Stresses, *Road Materials and Pavement Design,* Vol. 8, No. 1, pp. 61-86.

Appendix 1

Appendix 1 is comprised of two DVDs labeled as Appendix 1 (A) and Appendix 1 (B), respectively. Appendix 1 (A) includes 13 folders, and Appendix 1 (B) includes 12 folders. Each folder is labeled for a combination of tire load and tire inflation pressure. Each folder contains 1,200 pages of figures: 300 pages present pavement strains under the vertical stress component of the 3-D stresses; 300 pages illustrate pavement strains under the longitudinal stress component of the 3-D stresses; 300 pages display pavement strains under the transverse stress component of the 3-D stresses; and 300 pages show pavement strains under the combined 3-D stresses. In total, 30,000 pages of figures are included in DVD Appendix 1 (A) and DVD Appendix 1 (B).

These two DVDs are available upon request (at no charge) from Ms. Barbara Lorenz at the Southwest Region University Transportation Center. Ms. Lorenz's contact information is as follows:

Barbara Lorenz
Southwest Region University Transportation Center
Texas A&M University System
3135 TAMU
College Station, Texas 77843-3135
Phone: (979) 845-5815
Email: b-lorenz@tamu.edu

Appendix 2

Appendix 2 displays the pavement fatigue lives predicted by the Shell method. Although the predicted numbers of load repetitions are unreasonably large, they are plotted and listed in this appendix for reference.

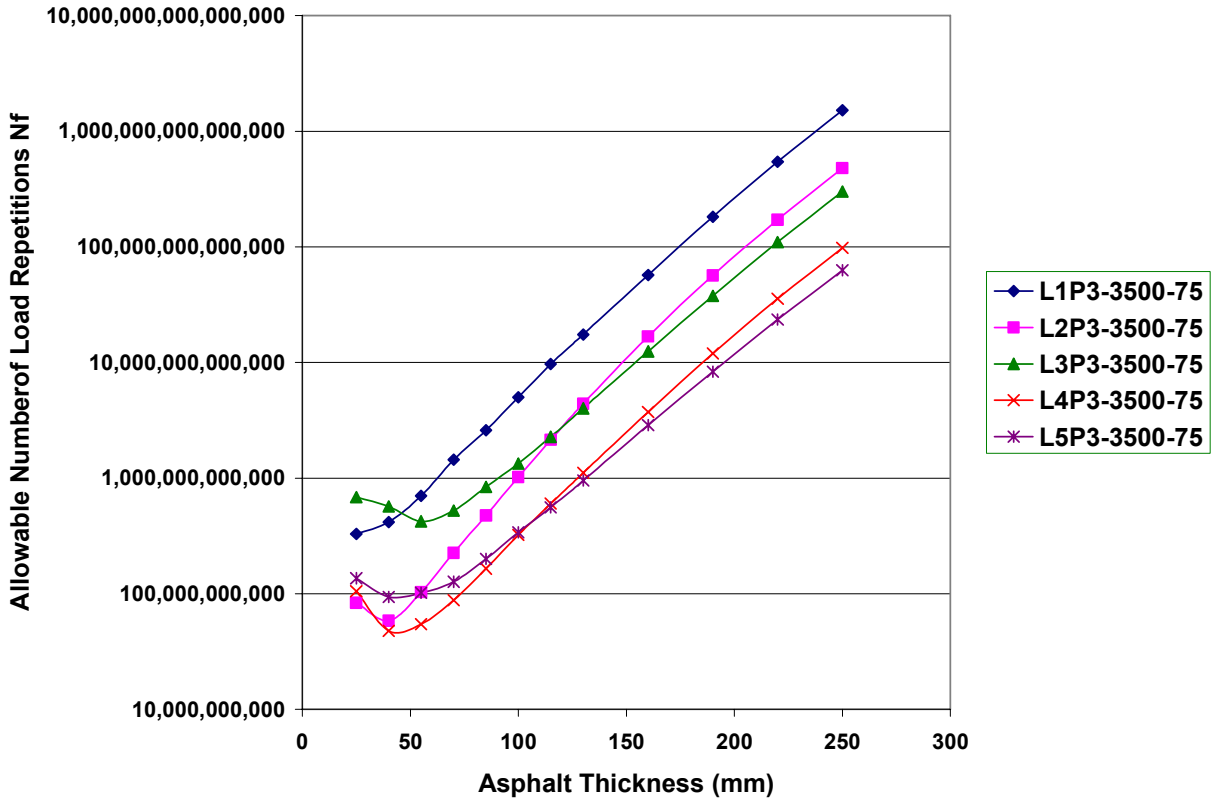

Figure 1. Effects of Tire Load on Pavement Fatigue Life Predicted by Shell Method Based on Tensile Strains Calculated by 3-D Stress Model

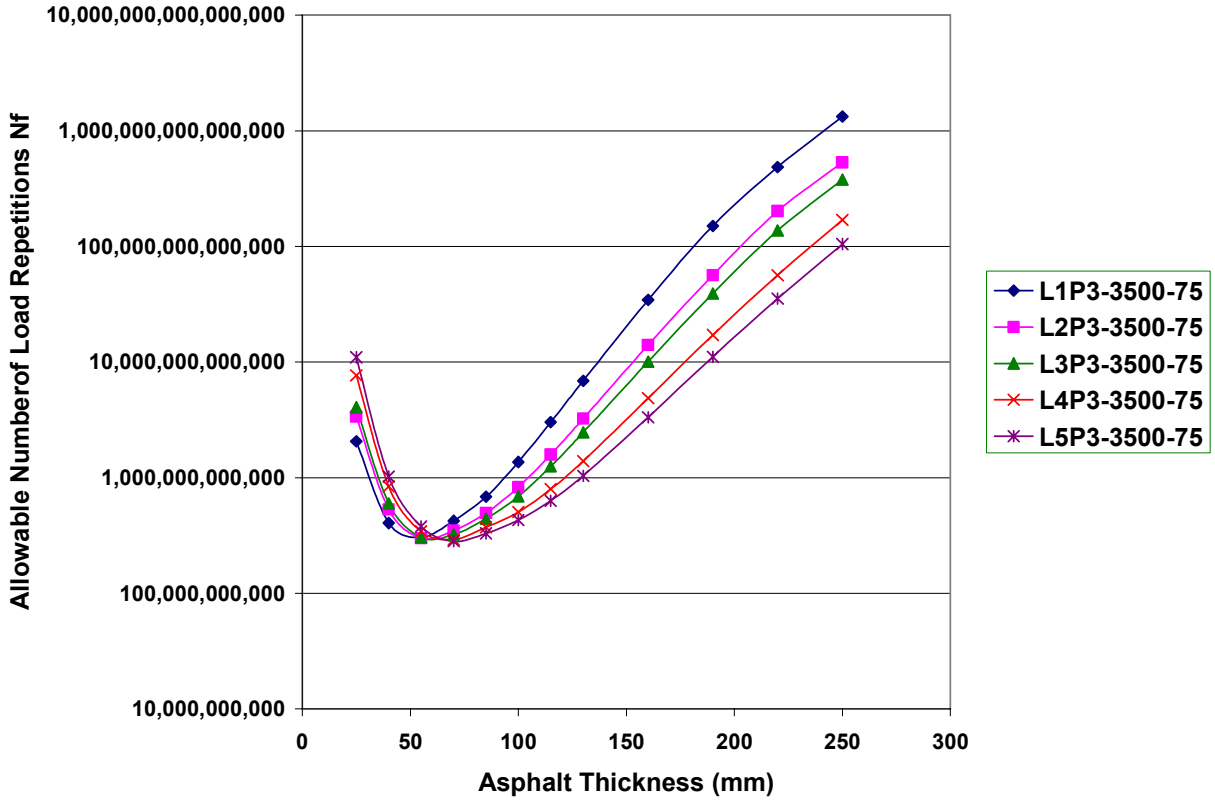

Figure 2. Effects of Tire Load on Pavement Fatigue Life Predicted by Shell Method Based on Tensile Strains Calculated by Uniform Stress Model

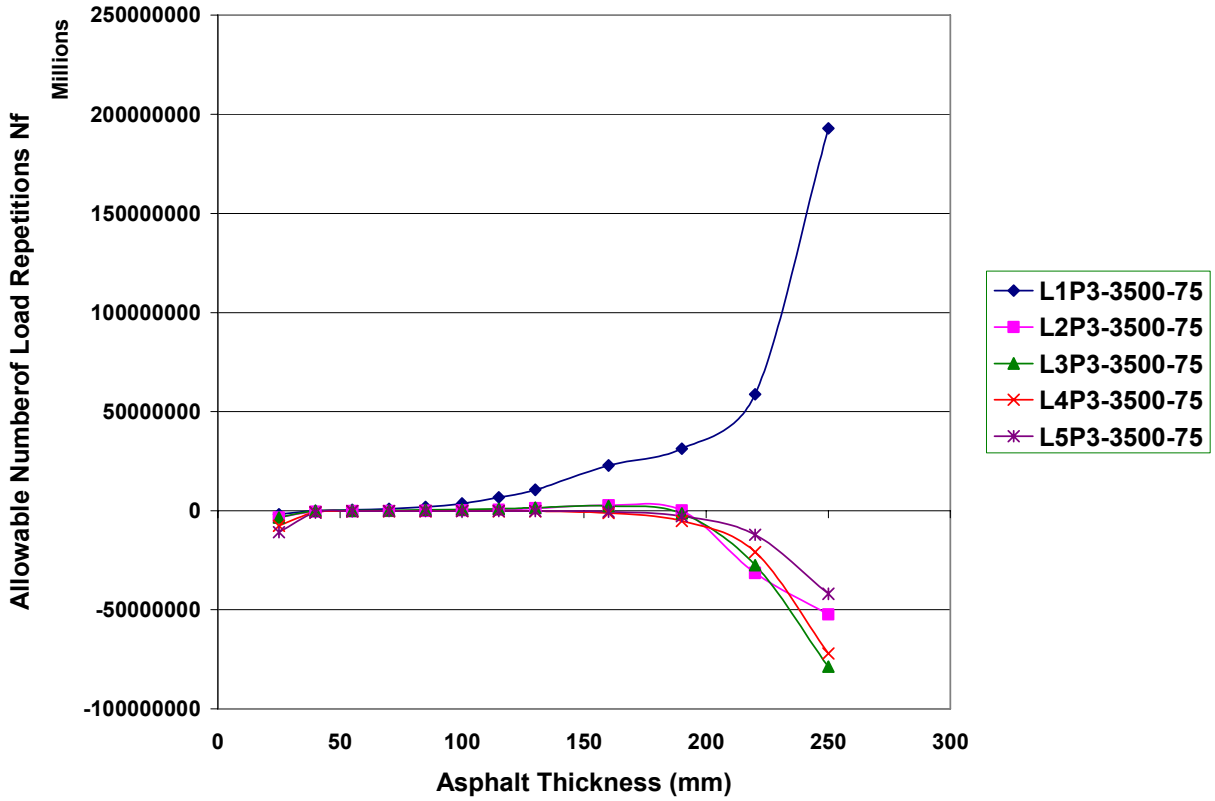

Figure 3. Differences in Number of Load Repetitions According to Differences in Tensile Strains Predicted by 3-D Stress Model and Uniform Stress Model (Varying Tire Load)

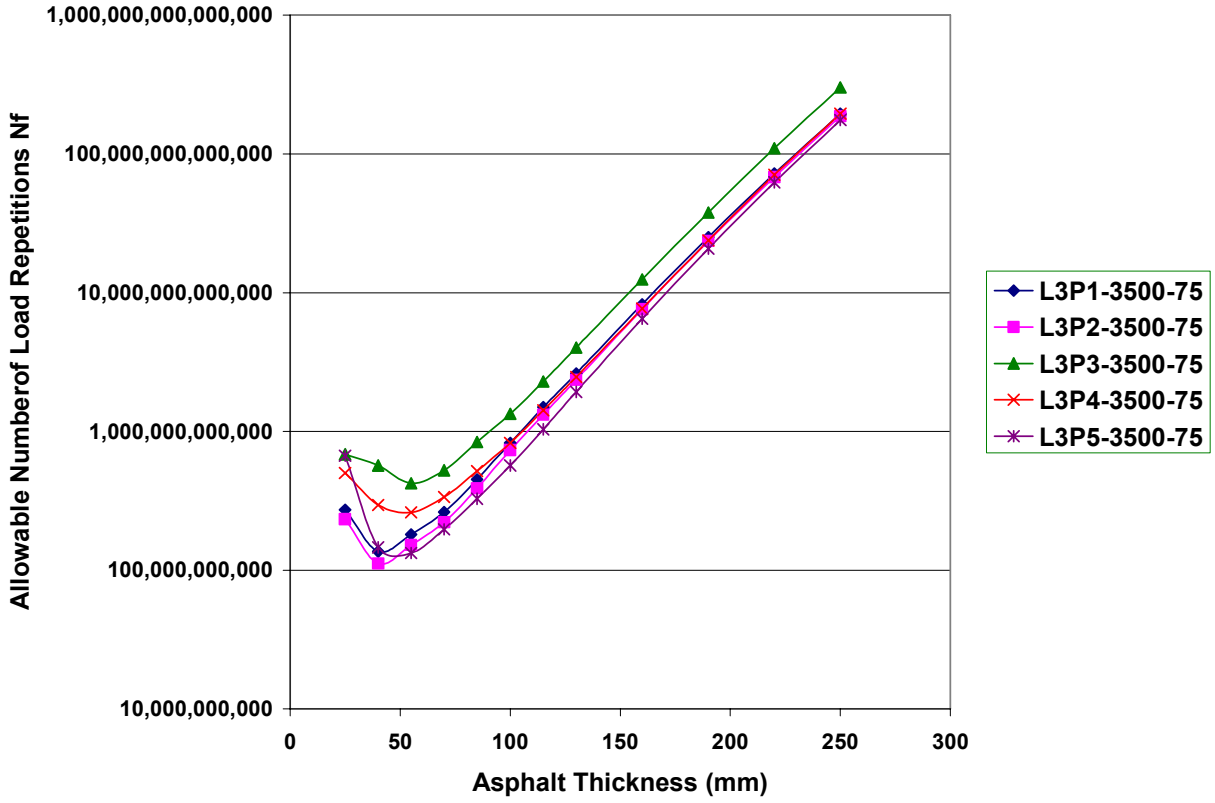

Figure 4. Effects of Tire Pressure on Pavement Fatigue Life Predicted by Shell Method Based on Tensile Strains Calculated by 3-D Stress Model

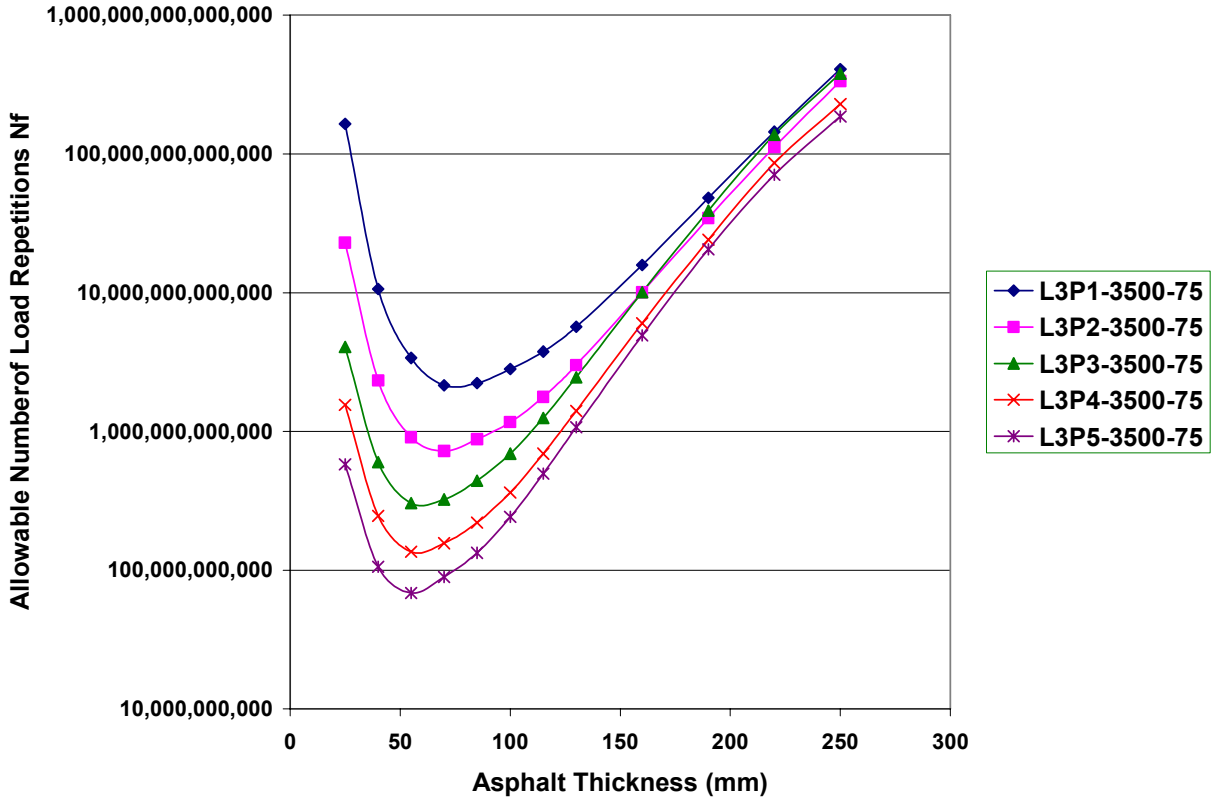

Figure 5. Effects of Tire Pressure on Pavement Fatigue Life Predicted by Shell Method Based on Tensile Strains Calculated by Uniform Stress Model

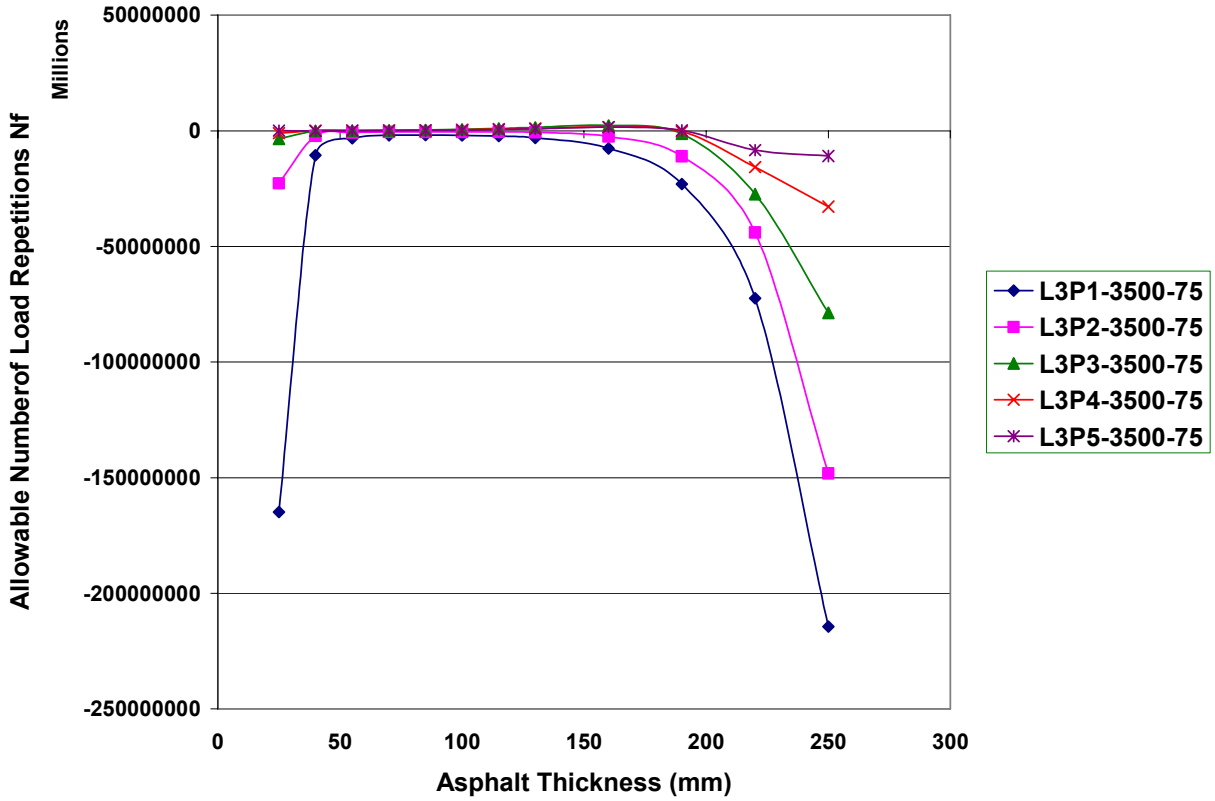

Figure 6. Differences in Number of Load Repetitions According to Differences in Tensile Strains Predicted by 3-D Stress Model and Uniform Stress Model (Varying Tire Pressure)

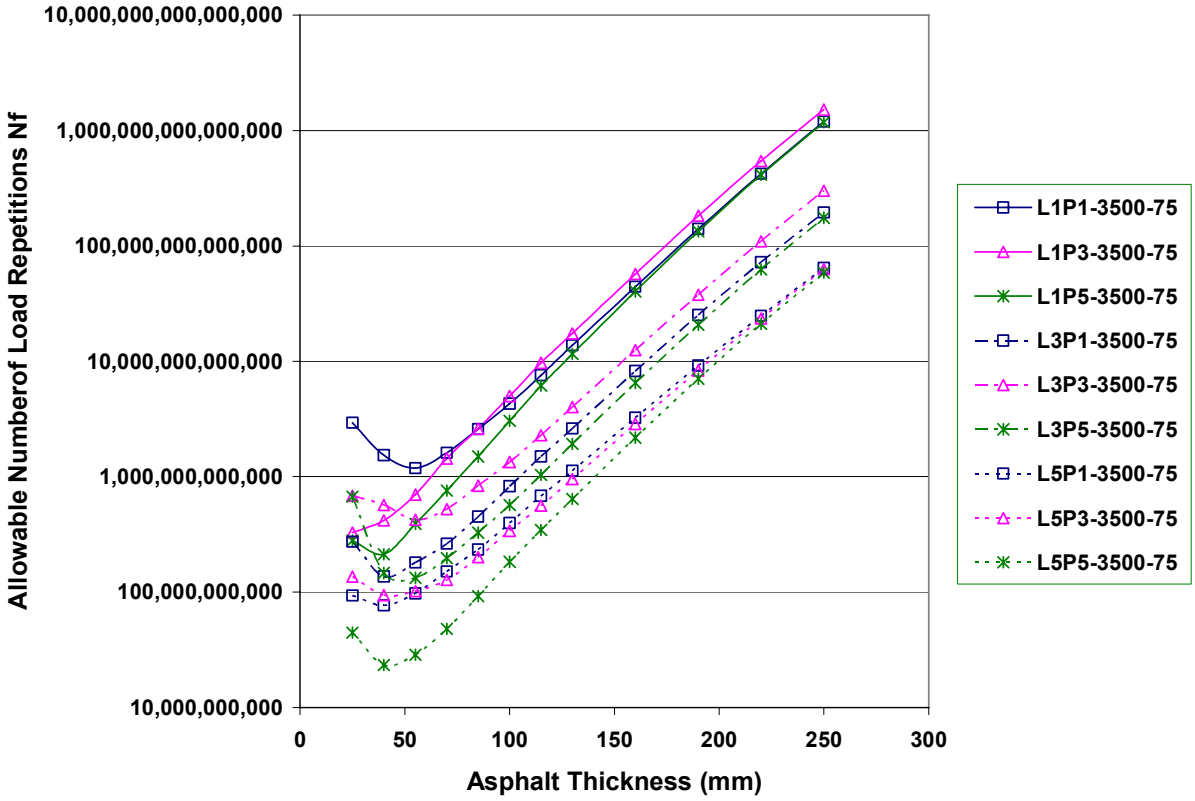

Figure 7. Effects of Tire Load and Tire Pressure on Pavement Fatigue Life Predicted by Shell Method Based on Tensile Strains Calculated by 3-D Stress Model

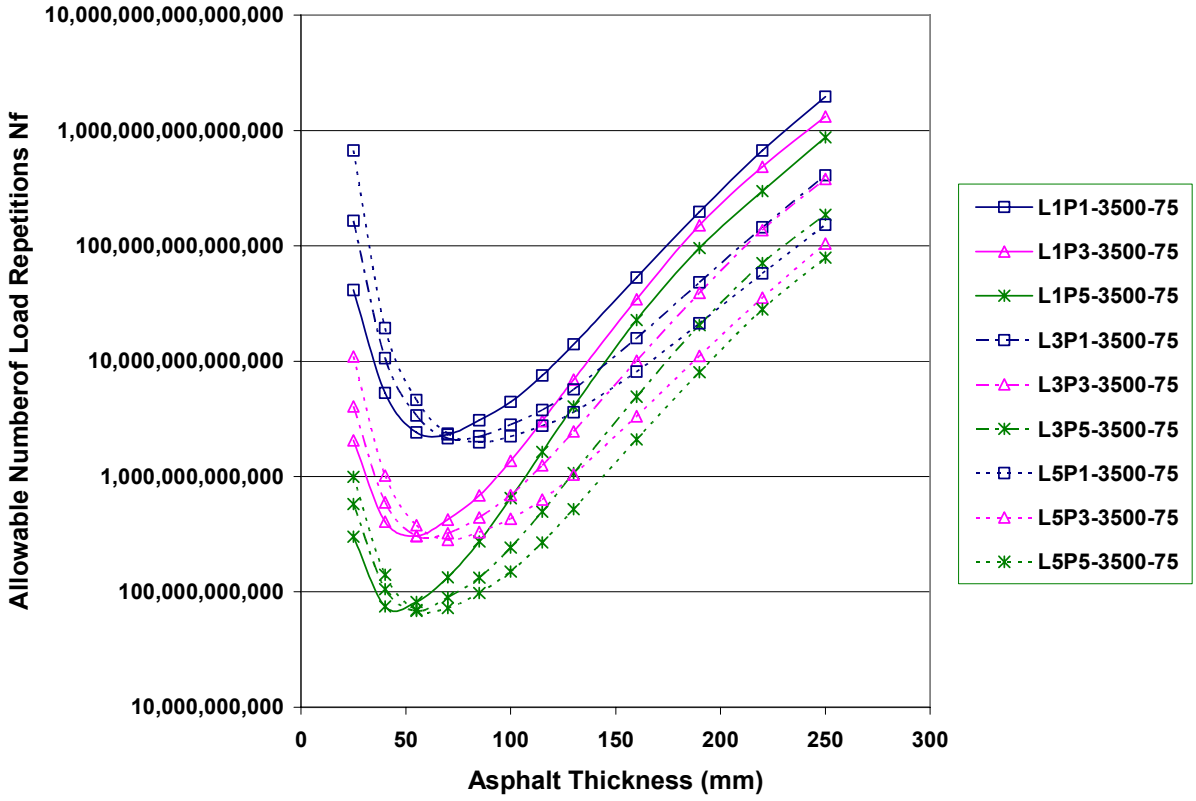

Figure 8. Effects of Tire Load and Tire Pressure on Pavement Fatigue Life Predicted by Shell Method Based on Tensile Strains Calculated by Uniform Stress Model

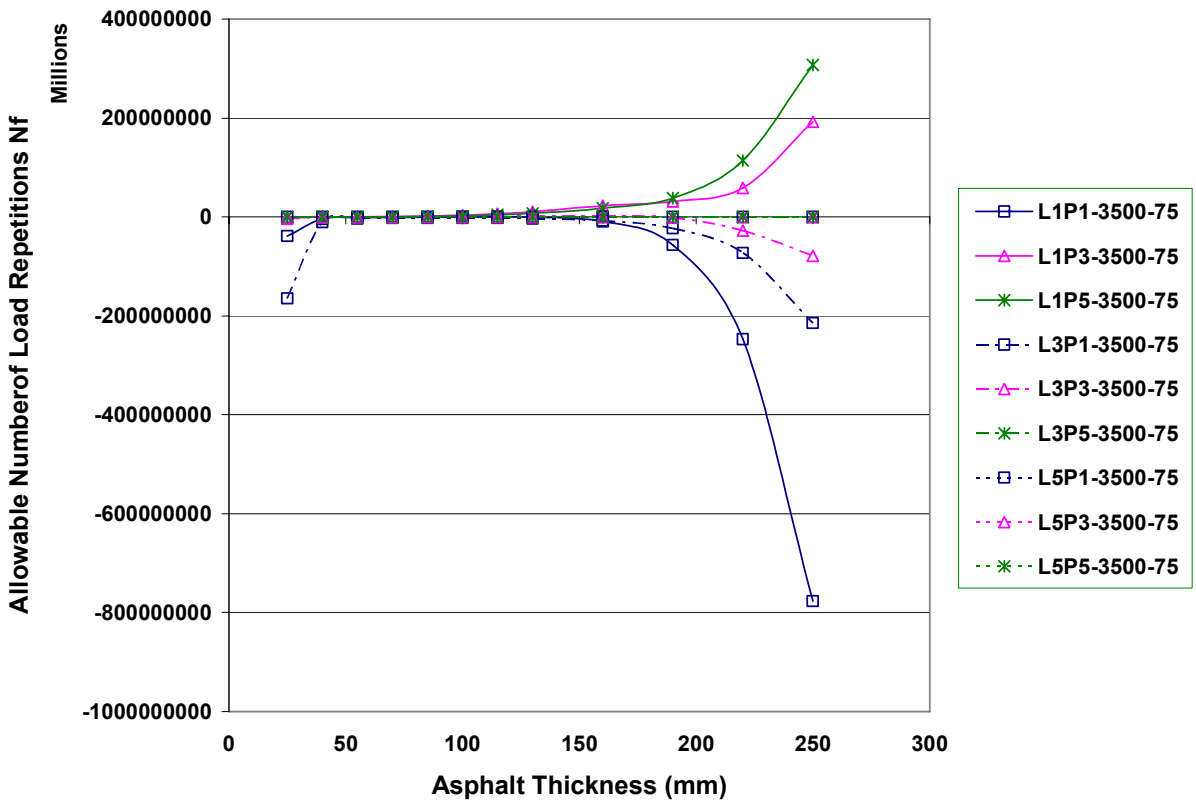

Figure 9. Differences in Number of Load Repetitions According to Differences in Tensile Strains Predicted by 3-D Stress Model and Uniform Stress Model (Varying Tire Load and Tire Pressure)